

Review

Enhancing Polylactic Acid (PLA) Performance: A Review of Additives in Fused Deposition Modelling (FDM) Filaments

Ioan Plamadiala ^{1,*}, Catalin Croitoru ^{1,*}, Mihai Alin Pop ² and Ionut Claudiu Roata ¹

¹ Materials Engineering and Welding Department, Transilvania University of Brasov, 500036 Brasov, Romania; ioan.plamadiala@unitbv.ro (I.P.); ionut.roata@unitbv.ro (I.C.R.)

² Department of Materials Science, Transilvania University of Brasov, 500036 Brasov, Romania; mihai.pop@unitbv.ro

* Correspondence: c.croitoru@unitbv.ro

Abstract: This review explores the impact of various additives on the mechanical properties of polylactic acid (PLA) filaments used in Fused Deposition Modeling (FDM) 3D printing. While PLA is favored for its biodegradability and ease of use, its inherent limitations in strength and heat resistance necessitate enhancements through additives. The impact of natural and synthetic fibers, inorganic particles, and nanomaterials on the mechanical properties, printability, and overall functionality of PLA composites was examined, indicating that fiber reinforcements, such as carbon and glass fibers, significantly enhance tensile strength and stiffness, while natural fibers contribute to sustainability but may compromise mechanical stability. Additionally, the inclusion of inorganic particulate fillers like calcium carbonate improves dimensional stability and printability, although larger particles can lead to agglomeration issues. The study highlights the potential for improved performance in specific applications while acknowledging the need for further investigation into optimal formulations and processing conditions.

Keywords: PLA; mechanical properties; additives; carbon fiber; glass fiber; additive manufacturing; graphene; CNT



Academic Editors: Vineet Kumar and Md Najib Alam

Received: 13 December 2024

Revised: 10 January 2025

Accepted: 12 January 2025

Published: 14 January 2025

Citation: Plamadiala, I.; Croitoru, C.; Pop, M.A.; Roata, I.C. Enhancing Polylactic Acid (PLA) Performance: A Review of Additives in Fused Deposition Modelling (FDM) Filaments. *Polymers* **2025**, *17*, 191. <https://doi.org/10.3390/polym17020191>

Copyright: © 2025 by the authors. Licensee MDPI, Basel, Switzerland. This article is an open access article distributed under the terms and conditions of the Creative Commons Attribution (CC BY) license (<https://creativecommons.org/licenses/by/4.0/>).

1. Introduction

The increasing demand for functional prototypes and end-use parts has driven the rapid development of Additive Manufacturing (AM) technologies, with Fused Deposition Modeling (FDM) or Fused Filament Fabrication (FFF) being one of the most popular methods. FDM relies on filaments, which are fed through a heated extruder and deposited layer-by-layer to create 3D objects. Choosing the right filament material is crucial for successful printing and achieving the desired final product properties. Over recent years, there has been growing interest in biopolymers as sustainable FDM alternatives to petroleum-based materials [1].

Among biopolymers, polylactic acid (PLA) stands out for its widespread production from renewable resources (240,000 tons annually) and its biodegradability and biocompatibility [2].

These qualities make PLA attractive for various applications, including commodity goods, medical devices, and FDM 3D printing [2]. PLA can be synthesized through several pathways, including condensation of lactic acid or ring-opening polymerization of lactide (its cyclic dimer) in the presence of tin octanoate or zinc stearate catalysts (Figure 1) [3].

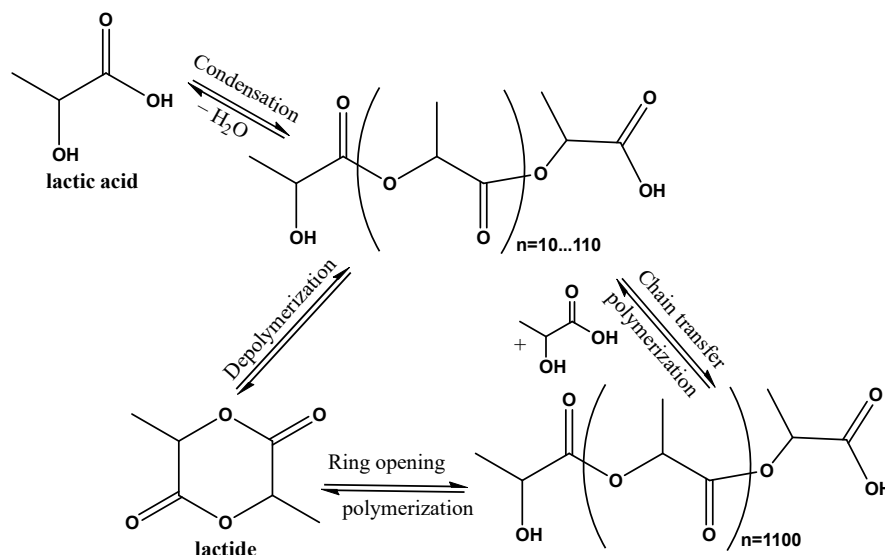


Figure 1. Main reaction pathways for polylactic acid (PLA) synthesis.

There is a noticeable upward trend in the total number of publications on PLA, as extracted from the Clarivate ISI Web of Science database (Figure 2), indicating increasing interest and research activity in this biodegradable polymer. Although the number of publications specifically involving PLA and 3D printing/FDM is less than the total PLA publications, it also shows a rising trend. This suggests that the use of PLA in 3D printing is gaining traction within the research community, especially since 2015. The growing number of publications could reflect advancements in PLA applications, improvements in 3D printing technology, and a broader recognition of the importance of sustainable materials. The same increasing trend could be seen in the number of studies involving 3D printing with custom-made (non-commercial) PLA filaments.

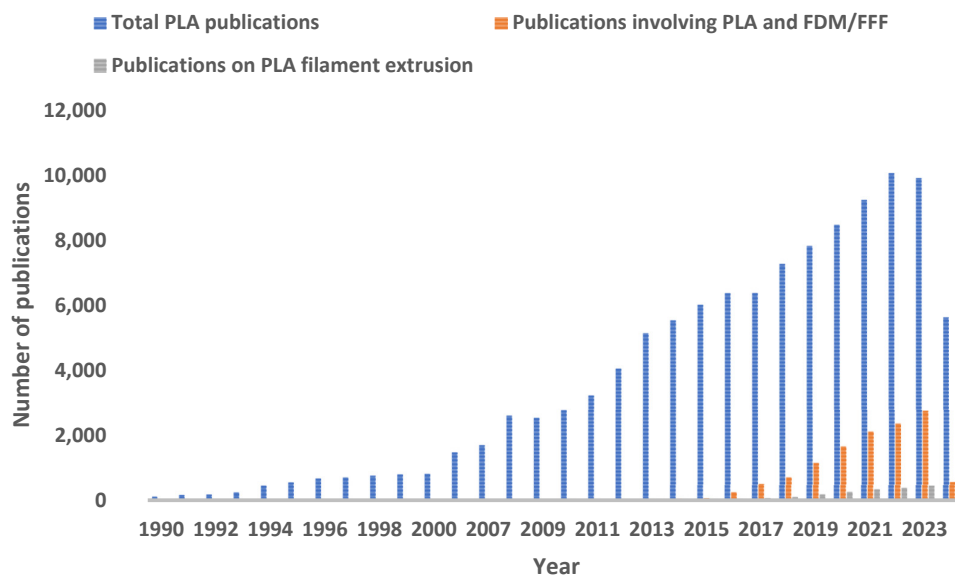


Figure 2. Number of publications involving PLA indexed in the Clarivate ISI Web of Science database (accessed on 2 January 2025).

PLA’s popularity in FDM stems from several advantages. First, its low melting temperature (150–180 °C) allows for easy printing and good layer adhesion, enabling intricate designs [4]. However, PLA also has limitations for FDM applications compared to other polymers, including those from the polyester class, such as polyhydroxybu-

tyrate (PHB), polybutylene succinate (PBS), polyethylene terephthalate glycol (PETG) or poly(acrylonitrile-co-butadiene-co-styrene) (ABS), as outlined in Figure 3 [5].

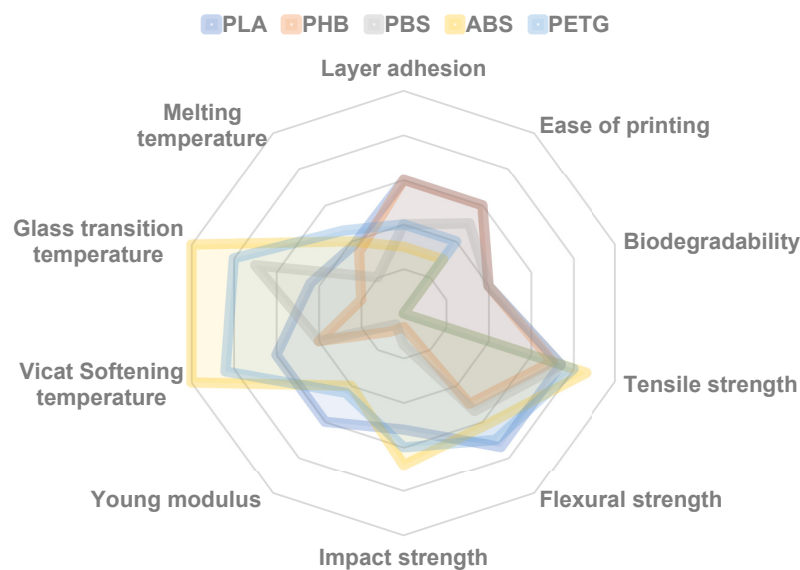


Figure 3. Main properties of commonly used fused deposition modeling (FDM) polymers in pure form (relative comparison) based on data from [6].

Compared to ABS or PETG, PLA has lower strength and heat resistance. Its heat deflection temperature (HDT) is 53–56 °C, meaning PLA parts can deform under elevated temperatures [5]. Additionally, PLA exhibits good tensile strength but lacks flexibility, making it unsuitable for load-bearing applications. Furthermore, PLA's high thermal expansion coefficient can cause warping and deformation during printing.

Additionally, PLA is not as strong or durable as other FDM materials to organic solvents (e.g., acetone, ethyl acetate, toluene, dichloromethane, aliphatic ketones), as the printed parts either dissolve or delaminate when exposed to these compounds. Also, more challenging alkaline/acidic conditions and humid environments can pose a problem, which may affect the longevity and performance of printed objects.

PLA's inherent limitations can be addressed through the incorporation of various fillers and additives into filaments. These can improve mechanical properties, thermal resistance, and printability.

While PLA is often praised for being an eco-friendly material in 3D printing, a deeper examination reveals a more nuanced picture. Typical PLA composite filaments for FDM applications go beyond just the reinforcing materials (like fibers or powders). They also include a surprising array of additional ingredients [7]. These additives, although necessary to achieve desired properties, can raise concerns about the overall environmental impact and efficiency [8–12]. The most important additives used in PLA filaments are the following:

- **Coupling Agents:** These improve the adhesion between the reinforcing material and the PLA matrix. Examples include silanes and maleic anhydride grafted polymers, with typical loading ratios of 0.5–3 wt. %
- **Impact Modifiers:** These additives enhance the toughness and impact resistance of the composite. They can be elastomeric polymers (e.g., thermoplastic polyurethane, TPU), core-shell particles, or other toughening agents, usually added in 5–15 wt. % ratios.
- **Processing Aids:** Lubricants (fatty acids or waxes at 0.5–3 wt. % loading) and plasticizers (e.g., poly (ethylene glycol) (PEG) at typical loadings of 5–10 wt. %) improve the flow and printability of the filament during printing.
- **Nucleating Agents and Antioxidants:** These additives promote crystallization, improve thermal properties, and prevent degradation of the PLA during processing

and use. Examples include talcum powder, calcium carbonate (1–5 wt. %), phenolic antioxidants, and UV absorbers (0.1–3%).

- Processing, since crystallinity results in poor dimensional stability due to shrinkage and
- Warpage in FDM processes.
- Flame Retardants: While these enhance safety, they often require high loading percentages, impacting printability and potentially adding weight (e.g., aluminum trihydroxide at 10–13 wt. %).
- Colorants: These add desired colors to the filament and printed parts without significantly affecting mechanical properties.

Despite the advancements, challenges remain in using additives with PLA for FDM printing. These challenges include compatibility issues between the additives, the filler material, and the PLA itself. Additionally, optimizing printing parameters and ensuring scalability of the manufacturing process are ongoing areas of research [3]. While these additives can improve mechanical performance, they may also lead to lower adhesion between layers compared to pure PLA. This is because faster solidification and larger voids can occur during printing with additives [13].

Future research should focus on overcoming these compatibility challenges and exploring the potential of PLA formulations with natural components for FDM printing [3]. A key area is achieving better dispersion of additives within the PLA matrix, which is crucial for optimal mechanical properties and avoiding defects in printed parts [3]. It is also important to consider the cost-effectiveness of additives, as some can be expensive and hinder biodegradability or the commercial viability of PLA filaments for certain applications [14].

Despite challenges like uneven printing, clogging, and filler–matrix distribution, natural fiber-reinforced PLA composites hold promise in addressing these issues [15], making the 3D-printed materials suitable for a wider range of applications [5,16]. For instance, adding cellulose-based fibers up to 30 wt. % can significantly increase PLA's stiffness and impact strength without impacting the density and environmental footprint of the material [17,18].

Researchers are pushing the boundaries of PLA's performance by exploring a wider range of fillers and reinforcements beyond natural fibers. This includes incorporating various synthetic fibers and particulate materials like metallic particles, ceramics, polymers or biomass-derived particles (e.g., sawdust). Metallic particles can enhance thermal conductivity, wear resistance, and electrical conductivity of PLA composites [19,20]. Certain iron or cobalt fillers can impart new properties in PLA, such as magnetic properties, which could be useful in sensor-based applications. However, achieving homogeneous dispersion and mitigating potential increases in weight and brittleness depending on the metal used are ongoing challenges. Similarly, ceramics can improve wear resistance, flame retardancy, and stiffness, but ensuring good dispersion and avoiding negative effects on printability and mechanical properties (the stress concentrator effect) require further research [21]. Both polymeric additives and biomass particles can significantly enhance the properties of PLA, making it more suitable for functional applications. Polymeric additives can improve toughness, and could strengthen the adhesion between PLA and reinforcing fibers [22].

Biomass particles, such as wood or micronized plant materials, can significantly increase strength, making PLA composites suitable for demanding applications [23,24].

Nanomaterial fillers offer even more exciting possibilities due to their high surface area-to-volume ratio. These materials have the potential to significantly improve properties like strength, flame retardancy, and barrier properties within PLA composites [25,26]. However, safe handling and proper integration of these materials within the PLA matrix necessitate further investigation.

This paper aims to provide an overview of the potential of PLA filaments filled with various reinforcing agents for FDM/FFF printing. The focus will be on how the incorporation of natural and synthetic fibers (like glass and carbon fibers), inorganic particles (such as calcium carbonate), organic biomass particles, nanomaterials or polymers can enhance the properties of PLA filaments. The advantages and disadvantages of these fillers/additives are discussed, focusing on their impact on mechanical strength, heat resistance, printability, and overall functionality of the printed parts. By examining the current state of research on filled PLA filaments, this paper aims to emphasize future developments in this field and promote the use of PLA for a wider range of FDM/FFF printing applications.

2. Reinforcing Agents for PLA FDM/FFF Applications

2.1. Fibers

In the realm of FDM 3D printing, PLA filament manufacturers have embraced the use of fiber reinforcements to elevate the material's mechanical properties and, in some cases, its environmental footprint. These reinforcements come in two main categories: synthetic and natural fibers.

Synthetic fibers, including carbon fiber, glass fiber, and Kevlar, are popular choices for reinforcing PLA due to their exceptional strength and stiffness. This translates to significantly enhanced mechanical properties in the resulting composites. They typically exhibit improvements in tensile strength, modulus, and impact resistance. For example, carbon fiber reinforcement can lead to a remarkable 150% increase in tensile strength, while glass fiber can boost the modulus by a range of 50–100%. Additionally, these synthetic fibers enhance the thermal stability and heat deflection temperature of PLA. Notably, carbon fiber can significantly improve thermal conductivity, making the composite suitable for high-temperature applications [27].

However, incorporating synthetic fibers presents a challenge in the filament extrusion process. Specialized equipment and techniques become necessary to ensure uniform fiber dispersion and prevent clogging during FDM printing.

Natural fibers like kenaf, hemp, flax, and bamboo are gaining traction as sustainable alternatives to synthetic fibers. Their biodegradability, renewability, and often lower cost align well with the eco-friendly nature of PLA. While not as dramatic as synthetic fibers, natural fibers enhance the tensile strength and modulus of PLA composites. Kenaf and hemp fibers, for instance, can increase tensile strength by 20–50%, with flax and bamboo offering similar improvements.

The sustainability benefits of natural fibers are undeniable. They are renewable, biodegradable, and have a lower environmental impact compared to their synthetic counterparts. Additionally, natural fibers are less expensive, making composites more affordable. They also offer a weight advantage, which can be crucial in applications where weight reduction is a priority.

However, natural fibers come with their own set of challenges. Their hygroscopic nature, meaning they tend to absorb moisture, can affect the mechanical properties and dimensional stability of the composites. This can be a significant drawback in applications where moisture resistance is critical. Furthermore, the properties of natural fibers can vary depending on factors like source, growing conditions, and processing methods. This variability can translate to inconsistencies in the performance of the final composites. Like synthetic fibers, incorporating natural fibers into PLA filaments can pose challenges during the extrusion and FDM printing processes, requiring careful attention to ensure uniform dispersion and prevent clogging. Some strategies that mitigate clogging are as follows:

- Using a large nozzle: Fibers can be larger than standard PLA fillers, so using a larger nozzle (e.g., 0.6 mm or 0.8 mm) can help prevent clogging.
- Printing at a higher temperature: Printing at a slightly higher temperature than standard PLA (around 200–220 °C) can help the fibers flow more easily through the nozzle.
- Reducing retraction: Minimizing retraction distance and speed can help prevent the filament from being pulled back into the nozzle, which can cause clogging.
- Adjusting printing speed: Printing at a slower speed can give the filament more time to melt and flow through the nozzle, reducing the risk of clogging.
- Drying the filament: Especially natural fibers can absorb moisture from the air, which can cause inconsistent extrusion and clogging.

2.1.1. Carbon Fiber

Carbon fiber-reinforced PLA (CFR-PLA) is one of the most popular composites. There are two main types of carbon fiber reinforcement: chopped and continuous. Chopped fibers, the most common option, are short lengths dispersed within the PLA, offering easier printing but with a lower reinforcement potential. Continuous fibers, embedded in a polymer sheath, provide the highest level of strength and stiffness but require specialized printers due to potential clogging and higher processing temperatures. The choice between these options depends on your priorities [28]. Chopped fibers are ideal for affordability and moderate improvements, while continuous fibers offer the best performance but necessitate a more advanced printing setup.

Typical fiber loadings range from 5% to 20% by weight. For instance, a study reported that 15% carbon fiber loading in PLA increased the tensile strength by over 100% compared to pure PLA [29]. Other studies conversely report reduced tensile strength but increased Young's modulus and elongation at break, for example, from 1.04 GPa and 6.26%, to 1.26 GPa and 7.81%, respectively [30,31]. The main weakness in these PLA-CF composites lies in the fiber–matrix interface, with fiber pull-out being the primary failure mode due to interface destruction. This effect is more pronounced at higher fiber loads reported to the PLA matrix [32].

The mechanical properties of 3D-printed carbon fiber PLA composite are significantly influenced by the FDM process parameters. The following parameters have been found to have a significant impact on the mechanical properties of CFR-PLA, as referenced from the literature [32–34]:

- Nozzle geometry: Square nozzle geometry increases tensile strength and reduces void geometry (with up to 7%) in carbon nanofiber-reinforced polylactic acid composites during FDM printing [35]. Also, this geometry enhances the fracture toughness with less inter-bead voids and larger bonded areas in carbon fiber-reinforced PLA composites [36].
- Printing Layer Height and print orientation: The layer height has a significant effect on the mechanical properties of CFR-PLA. A lower layer height (0.1–0.2 mm) can result in improved tensile strength and Young's modulus, while a higher layer height (0.4–0.6 mm) can lead to a decrease in mechanical properties [37]. A study mentions that a print orientation of 45° presents superior mechanical strengths [38]. Optimal process parameters for enhancing the impact strength of carbon fiber-reinforced PLA during FDM printing include layer thickness of 0.04 mm and shell thickness of 1.2 mm [39].
- Extrusion Width: The extrusion width has a significant impact on the mechanical properties of CFR-PLA. A wider extrusion width (0.4–0.6 mm) can result in improved

tensile strength and Young's modulus, while a narrower extrusion width (0.1–0.2 mm) can lead to a decrease in mechanical properties [32].

- **Printing Temperature:** The printing temperature has a significant effect on the mechanical properties of CFR-PLA. A higher printing temperature (230–250 °C) can result in improved tensile strength and Young's modulus, while a lower printing temperature (200–220 °C) can lead to a decrease in mechanical properties and lower dispersability of the fiber in the polymer melt [40]. Several studies indicate that the maximum tensile properties for carbon fiber-reinforced PLA are attained at a nozzle temperature of 230 °C [41,42]. Higher nozzle temperatures in the FDM process increase the crystallinity of printed PLA, promoting its nucleation, thus enhancing mechanical properties and rheological properties [13].
- **Printing Speed:** The printing speed has a significant impact on the mechanical properties of CFR-PLA. A slower printing speed (10–20 mm/s) can result in improved tensile strength and Young's modulus, while a faster printing speed (50–100 mm/s) can lead to a decrease in mechanical properties [38].
- **Infill Percentage:** Increasing the infill ratio in FDM printing increases the mechanical properties of both polylactic acid and carbon fiber-reinforced polylactic acid, with a maximum tensile strength of 35.65 MPa for PLA [43]. A higher infill percentage (50–70%) can result in improved tensile strength and Young's modulus, while a lower infill percentage (20–30%) can lead to a decrease in mechanical properties [44].

2.1.2. Glass Fiber

The addition of glass fibers (GFs) to 3D-printed PLA composites significantly enhances their mechanical and thermal properties. Optimal fiber content and innovative printing methods can further improve these properties, making GF-reinforced PLA composites suitable for a wide range of engineering applications. However, considerations such as moisture sensitivity and layer adhesion need to be addressed to fully leverage the benefits of glass fiber reinforcement.

- **Mechanical Strength Enhancement:** The addition of glass fibers significantly improves the tensile and flexural strength of PLA composites. For instance, composites with 30% glass fibers show superior mechanical properties compared to neat PLA. Continuous glass fiber reinforcement in PLA composites can achieve high flexural strength and modulus, reaching up to 312 MPa and 21.5 GPa, respectively [45–47]. The mechanical properties of PLA composites are optimized at specific glass fiber contents. For example, tensile strength and flexural strength are maximized at 20–30% glass fiber content, while impact strength peaks at 45% [45,48].
- **Thermal Stability:** GF addition enhances the thermal stability of PLA composites. Composites with 30% glass fibers exhibit excellent thermal stability, making them suitable for applications where thermal resistance is crucial. The heat deflection temperature and linear-expansion coefficient are significantly improved with the addition of short glass fibers [49]. Glass fiber-reinforced polylactic acid composites with isothermal heat treatment significantly improve mechanical properties and thermal stability, enabling their use in applications like automotive, aerospace, and electronics [50]. A study reported that PLA-GF composite filaments are thermally stable until 311 °C [51].
- **Layer Adhesion and Printability:** The incorporation of glass fibers can improve the printability and dimensional stability of PLA composites, although it may also lead to faster solidification and larger voids, which can affect layer adhesion [13,46].
- **Hygromechanical Properties:** Glass fiber-reinforced PLA composites exhibit anisotropic behavior, with better performance in the longitudinal direction compared to the trans-

verse direction. Moisture uptake can lead to a reduction in mechanical properties, particularly in the transverse direction [52].

- Chemical and structural stability: While glass fiber reinforcement in PLA (10–30% loading) significantly improves its strength and stiffness for demanding 3D printing applications, a study revealed interesting effects on weatherability. Compared to neat PLA, glass fiber-reinforced PLA (GF-PLA) showed improved mechanical properties even after exposure to sunlight and moisture (weathering). This is because the PLA itself degrades due to weathering, becoming weaker and developing cracks. Glass fibers, however, are much more stable and help the composite maintain its structural integrity. Even after extensive weathering, GF-PLA retains some mechanical advantages over neat PLA, thanks to the reinforcing effect of the relatively stable glass fibers [53].

Glass fibers often undergo a surface treatment, typically with a silane coupling agent, to improve adhesion with the PLA matrix. This enhances the stress transfer between the fibers and the polymer, leading to better mechanical properties in the final composite. Regarding the GF type and FDM process parameters, the most pronounced effects on the properties of the 3D-printed composites can be summarized as follows:

- The type and orientation of glass fibers in 3D-printed PLA composites significantly influence their mechanical and thermal properties. E-glass fibers are the most common and widely used due to their affordability, good balance of mechanical properties, and compatibility with various resins (including PLA). They offer good tensile strength, stiffness, and dimensional stability when incorporated into PLA filaments. Glass fibers for FDM/FFF applications typically come in diameters ranging from 6 microns to 20 microns. Thinner fibers offer better dispersion within the PLA matrix but may require higher loading percentages to achieve desired strength improvements. Conversely, thicker fibers can provide greater reinforcement but might be more challenging to disperse uniformly and could create printing issues like nozzle clogging.

Continuous glass fibers enhance longitudinal tensile strength but suffer from poor transverse properties due to anisotropic behavior. Short glass fibers (around 250 μm) improve thermal stability, making them ideal for thermally demanding applications. The presence and type of voids formed during 3D printing also play a crucial role in determining the composite's strength. Comparatively, 3D-printed composites may exhibit reduced mechanical performance compared to injection-molded ones due to differences in fiber orientation [46].

- Influence of Layer Thickness and Orientation: Thinner layers and specific orientations (e.g., flat orientation) improve tensile and flexural strengths. On-edge orientation with $+45^\circ / -45^\circ$ raster angles enhance mechanical strength and modulus [44].
- Extrusion rate and Temperature: Lower extrusion rates and higher printing temperatures improve mechanical properties by enhancing layer adhesion and reducing voids. The impact strength of the composite was found to decrease with increasing extrusion rate, from 2.5 kJ/m^2 to 1.5 kJ/m^2 when the extrusion rate was increased from 10 mm/s to 30 mm/s . A higher extrusion rate of 50 mm/s resulted in an impact strength of 1.2 kJ/m^2 [54,55]. The printing temperature has a significant impact on the mechanical properties of GF PLA composites. A study found that increasing the printing temperature from 190 $^\circ\text{C}$ to 230 $^\circ\text{C}$ resulted in a significant improvement in tensile strength and modulus of the composite. However, excessive printing temperatures can lead to warping and delamination of the composite. One study found that the printing temperature range of 230 $^\circ\text{C}$ to 240 $^\circ\text{C}$ resulted in a decrease in tensile strength by 1.02% and a decrease in elastic modulus by 3.32% [56]. Bed temperature also plays a

role, with higher bed temperatures (50–70 °C) improving crystallinity and mechanical properties [57].

- **Infill Density:** The infill density of the composite affects its mechanical properties. A study found that increasing the infill density from 10% to 50% resulted in a significant improvement in tensile strength and modulus of the composite [58]. Another study reported that an infill density of 30% yielded the highest tensile strength and modulus values [59]. A study found that samples with 50% and 75% infill density exhibited higher overall toughness compared to 100% infill density samples [51].

While glass fibers enhance tensile and flexural strength in PLA, they can make the printed parts more brittle, reducing their ability to withstand sudden impacts. Additionally, the abrasive nature of glass fibers can roughen the surface finish and accelerate wear on the printer's nozzle, requiring more frequent replacements [48].

2.1.3. Plant Fibers

Lignocellulosic fibers are derived from plant biomass (such as stems, leaves, seed husks and so on) and mainly consist of cellulose, hemicellulose, and lignin in various proportions. These natural fibers (NFs) are renewable, biodegradable, and have a low environmental impact. The most used lignocellulosic fibers in conjunction with PLA for FDM 3D printing include, for example, wood pulp fibers, cotton (lyocell), bamboo, sisal, jute, flax, sugarcane bagasse, ramie, henequen and hemp [60], although several other leaf-based materials are also considered (e.g., pineapple leaf fibers, microalgae). Typical fiber loadings used in 3D-printed PLA-based composites usually range from 1 to 10 wt. % [61].

NFs such as hemp, sisal, jute, flax, cotton or kenaf exhibit a range of mechanical and thermal properties that make them suitable for diverse applications. Hemp (*Cannabis sativa*) boasts high tensile strength (550–900 MPa) and good flexural strength (20–30 MPa), along with low moisture absorption (2–5%) and thermal conductivity (0.03–0.06 W/mK). Similarly, sisal (*Agave sisalana*) exhibits high tensile strength (400–600 MPa) and comparable thermal properties, including low density (1.3–1.5 g/cm³) and high thermal resistance (220–250 °C). Flax (*Linum usitatissimum*) shares these advantageous properties, with tensile strength reaching 500–700 MPa and extremely low moisture absorption (0.5–1.5%). Kenaf (*Hibiscus cannabinus*) also demonstrates impressive tensile strength (400–600 MPa) and thermal properties, low conductivity and high resistance up to 250 °C. In contrast, jute (*Corchorus capsularis*) and cotton (*Gossypium* spp.) exhibit moderate to low mechanical strength, with jute offering a tensile strength of 300–400 MPa and cotton 200–300 MPa, and both also suffer from high moisture absorption (10. . .20%) and lower thermal stability [62–66].

Lignocellulosic fibers are a natural, renewable, and readily available resource that offers several advantages as a reinforcement material for PLA in FDM 3D printing, such as sustainability, being a biodegradable and eco-friendly alternative to synthetic fibers like glass or carbon fiber, contributing to a more sustainable manufacturing process [67]. They also contribute to the overall composite weight reduction, having a lower density compared to many other reinforcing materials, leading to lighter-weight composites (ranging from 1.1 to 1.2 g/cm³, depending on the fiber type and content, neat PLA having an average density of 1.24 g/cm³). However, they also present some challenges, such as moisture absorption; lignocellulosics are hygroscopic, meaning they absorb moisture from the environment. The moisture absorption rate can vary from 1% to 15% by weight. This can negatively impact the dimensional stability and mechanical properties of the composite. The properties of the fibers can vary depending on the type of plant, harvesting time, age of the plant, processing methods, and growing conditions. This variability can affect the consistency of the final

composite material [68]. Some strategies for mitigation of these shortcomings are presented in the descriptive flow diagram from Figure 4 [69,70].

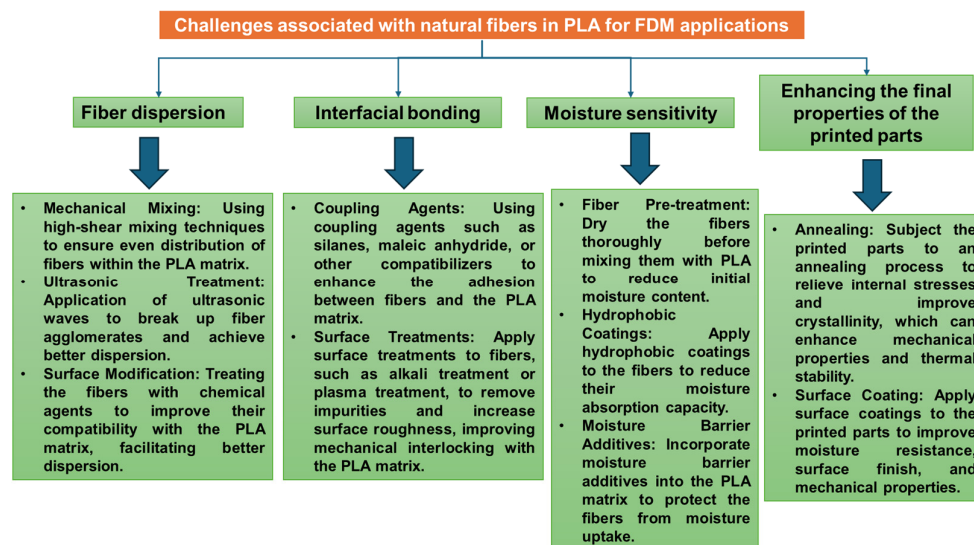


Figure 4. Flow diagram of challenges and mitigation strategies associated with the use of plant fibers in FDM applications.

Inhomogeneous fiber–matrix distribution in natural fiber-reinforced PLA composites for 3D printing remains a major challenge, along with uneven printing and clogging [71]. Plant fibers typically have lower surface energy than synthetic fibers, which can be modified through treatments to improve bonding with PLA. Surface treatments can be applied to lignocellulosic fibers to improve their compatibility with the PLA matrix and enhance the performance of the composite. Common surface treatment methods include [72]:

- **Alkali Treatment:** This treatment removes impurities, lignin and hemicellulose from the fiber surface, promoting better bonding with the PLA matrix and potentially improving mechanical properties [73].
- **Bleaching and pulping:** Natural fibers in their raw state harbor various impurities like waxes, oils, and lignin. These substances act as barriers, hindering the formation of strong bonds between the fiber and the PLA matrix. Pulping and bleaching processes effectively remove a significant portion of these impurities, particularly lignin. Lignin, a natural binder in plant cell walls, creates a weak interface with PLA. By eliminating lignin, pulping and bleaching create a cleaner fiber surface, allowing for better adhesion with the PLA matrix. These processes can slightly roughen the surface of the fibers. This increased surface area allows for better mechanical interlocking with the PLA, leading to a stronger bond and improved stress transfer between the fiber and the matrix [74,75]. Pulping and bleaching hemp fibers towards delignified short fibers significantly improves their compatibility with poly(lactic acid) and results in a 52% increase in tensile strength [76].
- **Silane Coupling Agents:** Silane coupling agents can create a chemical bond between the fibers and the PLA matrix, leading to improved interfacial adhesion and stress transfer, ultimately enhancing the mechanical properties of the composite [77].
- **Enzymatic modification:** Enzymatic-Assisted Modification of Thermomechanical Pulp Fibers Improves Interfacial Adhesion with Poly(lactic acid) via grafting of less hydrophilic moieties to the lignocellulose fiber surface, e.g., laccase-assisted grafting of octyl gallate (OG) or lauryl gallate (LG) onto the fiber surface [78].

Studies have shown that the inclusion of NFs in PLA can significantly influence the mechanical, thermal, and physical properties of the resulting composites [77].

- **Mechanical Properties:** Lignocellulosic fiber reinforcement can improve the tensile strength, modulus, and impact resistance of PLA composites. A study on the tensile behavior of 3D-printed PLA-based composites reinforced with natural henequen fibers found that the tensile strength and modulus increased with increasing fiber loading up to 5 wt. % [32]. Another study on lignocellulose nanofiber/poly(lactic acid) (LCNF/PLA) composites reported that the tensile strength and modulus increased with increasing fiber loading up to 10 wt. % [79]. Research has shown increases in tensile strength by 20–50% and modulus by 30–50% with the incorporation of wood fibers like kenaf and hemp [80]. The addition of natural fibers, such as wood, hemp, or flax, can improve the stiffness and strength of PLA composites. For example, a study found that the addition of 30 wt. % industrial hemp fibers to PLA increased the Young’s modulus by 10.9 Gpa and the tensile strength by 82.9 Mpa [73]. Natural fibers can also improve the toughness of PLA composites by increasing their resistance to crack propagation and improving their impact resistance [81]. The strength of 3D-printed kenaf/PLA composites increases to 3 wt. % but decreases significantly to 5 and 7 wt. % due to voids, and extrusion temperature affects the structure of the filaments [82].
- **Wear and friction:** NF-reinforced PLA composites exhibit reduced wear rates and friction coefficients, enhancing their suitability for tribological applications. Incorporation of natural fiber mats into the PLA matrix significantly improves wear behavior, resulting in a 10–44% reduction in friction coefficient and over 70% reduction in specific wear rate [83].
- **Thermal Properties:** The thermal stability of PLA composites with NFs can be slightly affected compared to neat PLA. Some studies report a decrease in the glass transition temperature (T_g) due to the presence of the fibers [84]. However, the thermal degradation temperature may not be significantly impacted.
- **Physical Properties:** NF reinforcement can decrease or increase the density of the composite compared to neat PLA, depending on fiber loading and type. Additionally, the hygroscopic nature of these fibers can affect the moisture absorption of the composite, potentially leading to dimensional changes.
- **Chemical and moisture stability:** PLA composites are more sensitive to high temperatures than to water. The mechanical properties, such as Young’s modulus, decrease significantly at elevated temperatures (80 °C), but the addition of natural fibers helps reduce this decrease [85].

Specifically, the typical mechanical and thermal stability properties of several natural fiber-reinforced PLA printed composites are given in Table 1.

Table 1. Comparison of mechanical properties of PLA composites reinforced with different types of natural lignocellulose fibers [data compiled from [86–88]]*.

Fiber Type	Tensile Strength (MPa)	Tensile Modulus (Gpa)	Flexural Strength (MPa)	Impact Resistance	Thermal Stability
Flax	50	5	60	High	Good
Jute	40	3	40	Medium	Medium
Sisal	30	2	30	Low	Low
Kenaf	45	4	50	Medium	Medium
Ramie	35	3	35	Low	Low
Cotton (lyocell)	25	2	25	Low	Low

* For comparison’s sake, the values corresponding to the mechanical properties were chosen as the median value for the respective composite type at the closest to 5 wt. % fiber loading.

Several fibers' structural properties and FDM process parameters play a crucial role in achieving good printability and the desired properties in NF-reinforced PLA composites [8,9]:

- Typically, fibers used in 3D printing are short fibers, often between 0.3 and 3 mm in length. Longer fibers can improve tensile strength but may cause issues with printability and nozzle clogging. The diameter of plant fibers can vary widely depending on the type of fiber. Common ranges are from 10 to 100 μm . Also, higher aspect ratio generally leads to better reinforcement. Typical aspect ratios for fibers used in 3D printing are between 50 and 200 [89].
- Printing Temperature: A higher printing temperature can improve the flowability of the PLA matrix and facilitate better fiber dispersion. However, excessively high temperatures can lead to thermal degradation of the wood fibers. The extrusion temperature for PLA-based composites containing lignocellulose fibers in FDM printing generally ranges between 200 °C and 220 °C. This temperature range plays a critical role in influencing the color, physical attributes, and mechanical properties of composites with heat-treated wood fibers, primarily due to changes in the chemical composition of lignocellulosic materials [77]. Research indicates that the PLA matrix in wood–plastic composite (WPC) parts remains amorphous during the FDM printing process, as the crystallization rate of PLA is too slow to achieve full crystallinity [90].
- Infill Pattern and density: The infill pattern can also affect the properties of the composites. A study on the 3D printing of PLA-based composites reinforced with natural lyocell fibers found that the tensile strength and modulus increased with the use of a concentric infill pattern compared to a grid or tri-hexagonal pattern [91]. Infill density significantly influences the improvement of mechanical strength in 3D-printed PLA composites with natural fiber reinforcement. Good tensile strength was observed at 25% of infill for flax fiber-reinforced 3D-printed composites [86]. Optimal load bearing is reported more often at filament crossing angles of $-45/+45^\circ$ [92].
- Build orientation: Generally, NF-PLA composite parts printed with the fibers aligned along the loading direction (e.g., on-edge orientation) exhibit higher flexural strength and modulus compared to parts printed with fibers perpendicular to the loading direction (e.g., flat orientation). The build orientation also influences the surface finish and the need for post-processing steps. For instance, printing a part with a smooth surface finish on the exterior layers can improve the flexural properties by reducing surface defects that could initiate cracks or failures. Additionally, post-processing techniques like annealing or heat treatment can be applied more effectively when the build orientation is considered, further enhancing the flexural properties of the composite part [93].

Also, Mansingh et al. [94] investigated the potential of fabricating fully biodegradable composites using an innovative 3D printing technique, with a particular focus on applications in food and medical product packaging. The weight percentage (wt. %) of powdered raw Pineapple Leaf Fiber (PALF) and alkali-treated PALF in the 3D-printed green composite presented a notable influence on its mechanical and thermal properties. Notably, the incorporation of 3 wt. % alkali-treated PALF yielded the optimal reinforcement, resulting in the highest tensile strength (42.9 MPa) and flexural strength (51.9 MPa). In contrast, composites reinforced with raw PALF exhibited superior ductility, achieving a maximum elongation at break of 6.89%. Additionally, the density of the 3D-printed composites increased proportionally with the wt. % of PALF content. The crystalline structure and chemical bonding characteristics of the composites were characterized through Fourier Transform Infrared (FTIR) spectroscopy and X-ray Diffraction (XRD) analysis. Microstructural analysis further revealed the presence of impurities, voids, and fiber degradation within the 3D-printed

composites. These findings underscore the influence of fiber treatment and composition on the performance and structural integrity of the green composites.

Several other studies involving the usage of fibers and PLA for 3D printing applications are summarized in Table 2.

Table 2. Composite filaments and 3D-printed materials involving PLA and fibers.

Reinforcement/Additive	Description	Properties	Applications	Reference
Cellulose nanofiber (CNF)	The CNF/PLA compounds were obtained by blending a PEG surface-modified CNF aqueous suspension with microscale PLA powder, followed by air-drying using various mass ratios of CNF to PLA, 0.25:99.75, 0.5:99.5, and 1:99, respectively.	Tensile strength 50.7 MPa, Young modulus E, 3.73 MPa	Environmentally friendly method which significantly reduced the use of chemical reagents and shortened the processing time.	[95]
steam-exploded coconut fiber (F) and PLA or PLA/PBS	PBS content: 0 or 20 wt. %; F content: 3, 6 or 10 wt. %	Impact strengths of PLA97/F3 and PLA77/PBS20/F3 were approximately 8.5% and 7.4% higher than those of the original PLA and PLA/PBS, respectively. During the degradation test, both PLA97/F3 and PLA77/PBS20/F3 exhibited higher tensile strengths than the original materials.		[96]
short lyocell fibers	Lyocell fibers (FCP400) with a nominal length of 400 μ m, loading reported to PLA: 10%, 20%, 30%	By combining fiber fibrillation, matrix modification, and post-printing annealing, we achieved an excellent balance of tensile strength (85 MPa), Young's modulus (7.2 GPa), and strain at break (3.2%)—the highest reported values for such composites.	performance structures using 100% bio-derived materials	[91]
Lignocellulose nanofiber/poly(lactic acid) (LCNF/PLA) composite	Cellulose raw material used was hardwood bleached kraft pulp (HBKP) with a degree of polymerization (DP _v) of ~750; cooking active alkali charges of 10%, 13%, 16%, and 19% (calculated by sodium oxide) with a liquor-to-chip ratio of 1:4.	The flexural strength of the CNF/PLA composite increased from 92.7 MPa to 151.2 MPa by combining 10% CNF (without lignin) with PLA. The flexural strength of LCNF/PLA composite with internal lignin content of 3.7% (0.37% of the total mass) was increased from 151.2 MPa to 234.5 MPa, which is 153.0% higher than that of pure PLA.		[79]
Carbon nanotubes (CNTs) were coated on short glass fibers (SGFs)	CNT-coated SGFs through a one-step flame synthesis technique. SGF- and CNT-SGF-reinforced composite filaments were fabricated with filler loadings of 1, 5 and 10 wt. %	Specimens using SGF- (≥ 5 wt. %) and CNT-SGF (1–5 wt. %)-reinforced PLA filaments exhibited higher Young's modulus and tensile strength values due to the enhanced interface adhesion. Furthermore, the FDM printing raster angles ($\pm 45^\circ$ and $0^\circ/90^\circ$) did not noticeably affect the tensile properties of the samples made of the same material.		[97]

2.2. PLA Reinforced with Particles

Some common examples of particle reinforcements for Poly(lactic acid) (PLA) used in FDM 3D printing, along with their properties and typical loading weights, are as follows:

- **Calcium Carbonate (CaCO₃):** This is a widely used mineral filler for PLA. It is inexpensive, abundant, and can improve the stiffness, dimensional stability, and printability of PLA. For example, adding 20–30% by weight of CaCO₃ particles can increase the modulus and heat deflection temperature of PLA while also improving layer adhesion. A specific product is Omycarb TF-100, a fine ground calcium carbonate with a median particle size of 1.3 microns, which can be added at 20–30% by weight. A study in

the Journal of Polymers and the Environment found that adding 20% CaCO₃ to PLA increased its flexural modulus by 50% and reduced its thermal expansion coefficient by 30%.

- **Carbon Black:** Carbon black particles can be used to improve the electrical conductivity and mechanical properties of PLA. They are typically added at a loading weight of 1–10%. For example, a research paper in the Composites Science and Technology journal reported that adding 5% carbon black to PLA increased its electrical conductivity by several orders of magnitude and its tensile strength by 20%.
- **Talcum (Magnesium Silicate):** Talc is a soft, lamellar mineral that can act as a reinforcing agent and nucleating agent in PLA. It improves stiffness, impact strength, and heat resistance of PLA. For instance, adding 10–20% by weight of talcum particles can enhance the dimensional stability and surface finish of printed parts. An example is Luzenac Talc, which has a median particle size of 1.5 microns and can be added at 10–20% by weight.
- **Nanoclay:** Nanoclays, such as montmorillonite, are commonly used to improve the barrier and mechanical properties of PLA. They act as nano-scale reinforcements, increasing stiffness, strength, and heat resistance. For example, Cloisite 30B, an organic-modified montmorillonite nanoclay, can be added at 5–10% by weight to PLA to improve its gas barrier properties and mechanical strength. For instance, adding 3% nanoclay to PLA increased its tensile strength by 25% and its flexural modulus by 35% [98].
- **Silicon dioxide (SiO₂):** Silicon dioxide particles, also known as silica, can be used to improve the toughness and impact resistance of PLA. They are typically added at a loading weight of 1–5%. For instance, a research paper in the Journal of Applied Polymer Science reported that adding 3% silica to PLA increased its impact strength by 50% and its elongation at break by 100%.
- **Metal Powders:** Metal particles, such as copper or brass, can be added to PLA to create metallic-looking prints with improved mechanical properties. These particles increase the weight, density, and stiffness of the printed parts. For example, adding 5–15% by weight of brass powder with a particle size of 35–45 microns can create a brass-infused PLA with a metallic sheen.

2.2.1. PLA with Calcium Carbonate

CaCO₃ is a naturally occurring mineral that exists in several crystalline forms, including aragonite, calcite, and vaterite [99,100]. These polymorphs have different crystal habits, particle sizes, and surface areas, which can influence the final properties of the PLA filaments [101]. The use of CaCO₃ particles in PLA filaments can improve their mechanical properties, such as tensile strength and flexural strength, by acting as a reinforcing material [101,102]. Additionally, CaCO₃ can enhance the thermal stability and resistance to degradation of PLA filaments [101]. Also, this type of composite is researched as a potential biomaterial (ceramic-coated scaffolds), showing potential for further evaluations in bone tissue engineering applications [100]. Regarding the structural and morphological characteristics of calcium carbonate, several parameters influence the properties of the 3D-printed composites [103]:

- **Morphology:** The morphology of the CaCO₃ particles, such as spheroidal (granular) or rod-like (Figure 5), can also impact the mechanical properties of PLA filaments. Rod-like particles, for example, have been found to have a more pronounced influence in improving mechanical properties compared to spherical particles. Particles with higher specific surface areas tend to agglomerate more within the PLA matrix, leading to a decrease in mechanical properties [104]. A critical value for the specific

surface of calcium carbonate in correlation to PLA was not determined, but as an orientative value, it is around $7 \text{ m}^2/\text{g}$ for polyolefin matrices, beyond which increased agglomeration causes a significant decrease in strength and impact resistance [105].

- Amorphous calcium carbonate (ACC) derived from various sources, such as limestone (LS), chalk, or animal origins like white eggshells (WESs), has been explored as a filler material for polylactic acid (PLA) composites. These fillers are particularly beneficial due to their potential to enhance the mechanical properties of PLA-based materials. Notably, the particle size of the ACC plays a significant role in the resulting composite's performance. Studies have shown that fillers with a particle size of $32 \mu\text{m}$ tend to exhibit superior tensile strength compared to those with a larger particle size of $63 \mu\text{m}$. This suggests that smaller particles contribute more effectively to the reinforcement of the PLA matrix, likely due to their higher surface area, which facilitates better interaction with the polymer matrix. In addition to tensile strength, the tensile modulus of PLA composites is significantly influenced by the filler content. For amorphous calcium carbonate-based fillers, the tensile modulus increases as the filler content rises, indicating enhanced stiffness and structural integrity. The highest tensile modulus was observed at a filler content of 20 wt. % for both $32 \mu\text{m}$ and $63 \mu\text{m}$ particle sizes, suggesting that this concentration represents an optimal balance between filler loading and the material's mechanical properties. When comparing the toughness of different ACC sources in PLA composites, it was found that limestone (LS)-based fillers provided superior toughness compared to those derived from white eggshells (WESs). This difference in toughness is likely due to variations in the microstructure and the intrinsic properties of the fillers, which influence the energy absorption capacity of the composite materials. Overall, the use of amorphous calcium carbonate fillers, particularly from limestone, shows promising potential in improving the mechanical performance of PLA composites, offering a viable option for enhancing the material's strength and durability for various applications [106].

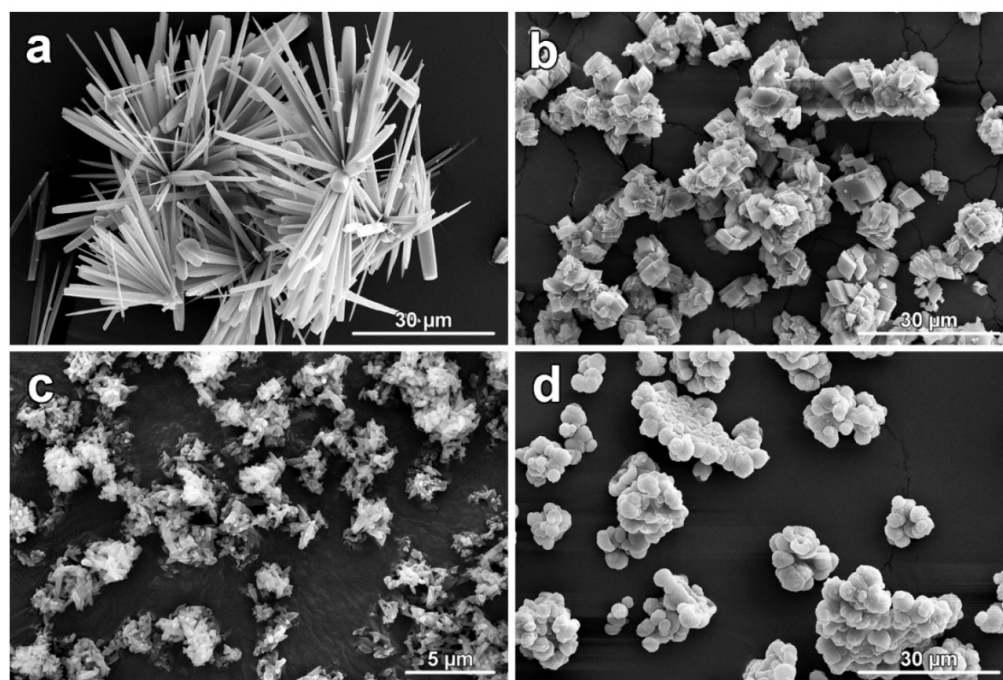


Figure 5. Collection of observed morphologies of synthesized CaCO_3 polymorphs (aragonite (a), calcite (b), commercially available calcite (c), and vaterite (d)) observed under SEM [distributed under the terms and conditions of the Creative Commons Attribution (CC BY) license <https://creativecommons.org/licenses/by/4.0/>, accessed on 13 June 2024, from [104]].

The processing parameters for printing PLA-CaCO₃ composites, referenced from the literature, are as follows [107–109]:

- Nozzle Temperature Optimal Range: 190 °C to 210 °C. Higher temperatures can improve the dispersion of CaCO₃ particles within the PLA matrix, improving the mechanical properties.
- Printing Speed: 50 to 80 mm/s. Slower speeds can lead to better particle dispersion and improved mechanical properties.
- Infill Density: 50% to 80%. Higher densities can enhance the mechanical properties of the printed part, especially with higher CaCO₃ loads.
- Infill Pattern: Use a grid or honeycomb pattern for better stress distribution and to take advantage of the improved stiffness of PLA-CaCO₃ composites.
- Layer Height: 0.1 to 0.3 mm. Fine layers can improve the surface finish and mechanical properties, especially with high-quality prints.

A low-permeability polylactic acid (PLA) coating to calcium carbonate (CaCO₃) microparticles was successfully applied, which encapsulated co-precipitated bovine serum albumin-fluorescein isothiocyanate (BSA-FITC), utilizing the solvent/oil/water (S/O/W) emulsion technique (Figure 6) [110,111]. This effectively sealed the micro-particle pores and significantly decreased the shell permeability. The incorporation of an additional polyvinyl alcohol (PVA) layer significantly improved the stability of the coated microparticles and refined the size distribution of the resultant PLA/CaCO₃ particles. The formulation of the particles was optimized with a PVA concentration of 2.5%, which was found to be the most effective for achieving a stable and uniform particle size distribution. To gain a deeper understanding of particle formation, the varying mass ratios of CaCO₃ microparticles to PLA were systematically examined across different samples. Bovine serum albumin-fluorescein isothiocyanate (BSA-FITC) was observed within the PLA particles across all formulations, with the CaCO₃/PLA mass ratio ranging from 0.1 to 1.2. At CaCO₃/PLA mass ratios below 0.8, the polymer-coated microparticles exhibited increased resistance to ethylenediaminetetraacetic acid (EDTA) treatment, thereby maintaining the integrity of their bioactive cargo. In contrast, at a CaCO₃/PLA mass ratio of 1.2, the PLA-coated particles displayed increased susceptibility to EDTA due to the thinner PLA coating on each CaCO₃ particle and the presence of pores in the PLA shell. This compromised the stability of the bioactive content within the particles. Based on these findings, a CaCO₃/PLA mass ratio of 0.8 was determined to be optimal, as it provided the highest protein payload while maintaining the stability of the microparticles against dissolution. This ratio offers a favorable balance between bioactive content retention and the structural integrity of the particle coating.

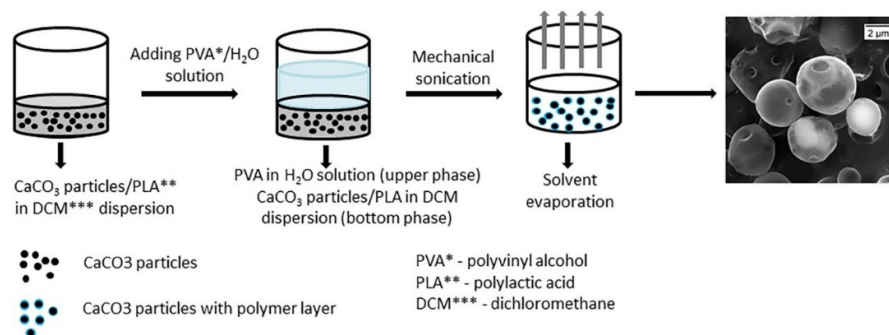


Figure 6. Fabrication of PLA CaCO₃ hybrid micro-particles [reproduced with permission from [111].

Both PLA and CaCO₃ are biodegradable materials [112], making them highly suitable for biomedical applications. Given that CaCO₃ is a natural component of bone, this microcapsule system holds potential for the storage and controlled delivery of bone growth

factors or other pharmaceutical agents aimed at treating bone-related diseases. Additionally, the system could provide enhanced mechanical support during cargo delivery. Advanced delivery strategies, such as targeted drug delivery, could be realized by incorporating magnetic nanoparticles into the PLA shell. This modification would enable magnetic navigation, allowing precise delivery of drug-loaded microcapsules to specific target sites. The PLA-coated CaCO_3 microparticles, encapsulating bioactive molecules, are anticipated to have diverse applications in biomedicine, particularly as efficient drug storage and delivery systems. Furthermore, the hybrid microcapsules developed in this study could be employed for the encapsulation of a wide range of water-soluble substances, including proteins, insulin, cytostatics, and polysaccharides. This versatility underscores the potential of these microcapsules as a multifunctional platform for various therapeutic and pharmaceutical applications

2.2.2. PLA with Zinc Oxide

Poly(lactic acid)-Zinc Oxide (PLA-ZnO) nanocomposites have emerged as versatile and multifunctional materials, suitable for a wide array of applications due to their exceptional antibacterial, photocatalytic, and ultraviolet (UV) absorption properties. Their superior antibacterial performance offers a significant advantage over pure polymers by reducing the risk of infection through fomite transmission. Despite these promising attributes, the current utilization of PLA-ZnO nanocomposites, predominantly produced via conventional fabrication methods, remains limited to simple geometries such as films and fibers. To date, few studies have explored the additive manufacturing (AM) of PLA-ZnO nanocomposites, primarily due to challenges in material processing and the production of filaments with properties that can be reliably preserved post-3D printing [113].

As research advances to overcome these challenges, the integration of PLA-ZnO nanocomposites into AM has the potential to expand their application spectrum significantly. AM offers a distinct advantage in fabricating complex geometries and customized components, which could unlock novel uses for these nanocomposites. This intersection of 3D printing with advanced antibacterial materials is garnering increasing interest within the biomedical field, with the goal of creating personalized antibacterial medical devices tailored to individual patient anatomies. Furthermore, this innovation aligns with the priorities of the post-pandemic AM industry, aiming to deliver safer and more hygienic materials for enhanced environmental security. Nevertheless, a critical concern is whether the functional properties of PLA-ZnO nanocomposites, particularly their antibacterial effectiveness, can be retained at sufficient levels after undergoing the AM process. The transition from conventional manufacturing to AM introduces additional processing steps, such as high-temperature extrusion and deposition, which may alter the intrinsic properties of the nanocomposite materials. Understanding the impact of these processes on the structural integrity and functionality of PLA-ZnO nanocomposites remains a key research focus, as it will determine the feasibility of their broader implementation in additive manufacturing [114].

2.2.3. PLA with Silicon Carbide and Graphite

Silicon carbide (SiC) and graphite are chosen as fillers for poly(lactic acid) (PLA), primarily due to their mechanical and thermal attributes. A significant reduction in recovery time is observed for composites with high filler loading. For instance, a composite comprising 50 wt. % carbon and 10 wt. % SiC in a PLA matrix exhibits an 87% decrease in recovery time compared to pure PLA [115]. The evaluation of shape recovery performance is based on three key parameters: recovery ratio, recovery rate, and recovery time. The recovery ratio is defined as the proportion of the initial deformation angle restored after the recovery

process. The recovery rate represents the instantaneous time derivative of the recovery ratio, providing insight into the speed of shape restoration. Recovery time is measured as the interval between the initiation of the thermal trigger and the point at which the recovery rate reaches its maximum value. A detailed methodology for the extrusion of printer filaments and the subsequent 3D printing process is thoroughly described to ensure reproducibility and clarity.

By altering the material composition, and consequently its thermal conductivity, the rate of shape memory response can be effectively controlled. The correlation between material composition and shape recovery rate, determined through thermal conductivity analysis, offers a framework for designing structures capable of activating shape memory responses at tailored rates. The advanced capabilities of 3D printing, particularly the use of multiple filaments and print heads, enable the fabrication of structures with highly heterogeneous material compositions. This approach represents a significant departure from conventional methods, such as variations in temperature or structural thickness, that have traditionally been used to modulate the timing of shape memory response activation within structures.

Several mechanical properties (UTS: ultimate tensile strength (MPa); strain at break (%); flexural strength (MPa) and impact strength (kJ/m^2)) of 3D-printed PLA reinforced with various inorganic fillers selected from the literature are given in Figure 7. In this figure, the average value was calculated from the samples sets presented in the indicated studies.

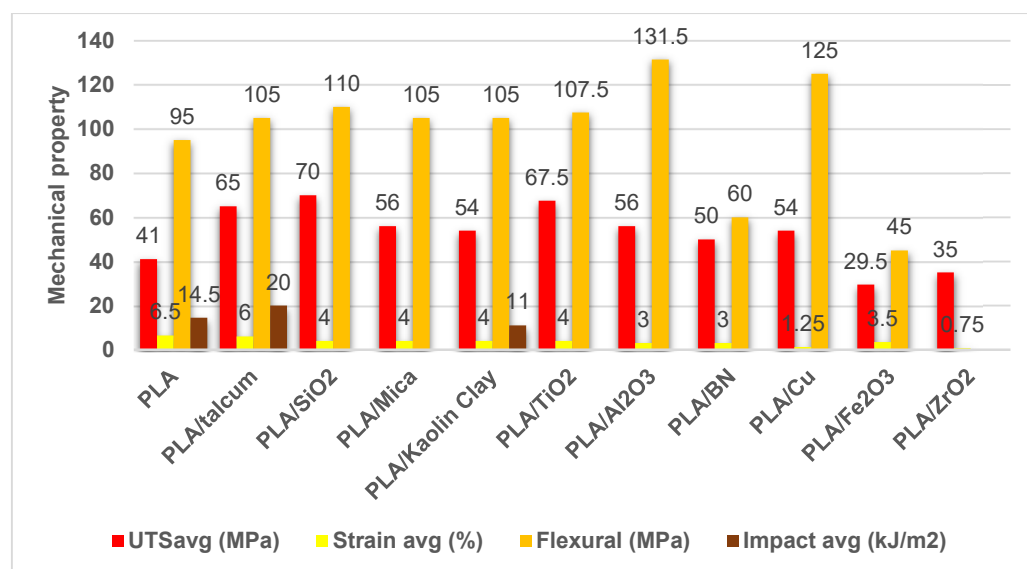


Figure 7. Average values for the mechanical properties of 3D-printed PLA reinforced with inorganic additives: neat PLA [116]; talcum [117,118]; silica (SiO_2) [119,120]; mica [121,122]; kaolin clay [123]; titania (TiO_2) [124,125]; alumina (Al_2O_3) [126]; boron nitride (BN) [127]; copper (Cu) [128]; iron (III) oxide (Fe_2O_3) [129]; zirconia (ZrO_2) [130].

Overall, the inclusion of various fillers, such as, notably, titanium dioxide (PLATiO₂) and copper (PLA/Cu), appears to improve the mechanical properties of the PLA material compared to the baseline PLA without any fillers.

2.3. PLA Reinforced with Carbon-Based Nanomaterials

The most effective nanomaterials for enhancing the mechanical properties of PLA in FFF/FDM 3D printing are [131–133]:

- Carbon nanotubes (CNTs): Several studies have shown that incorporating CNTs into PLA can significantly improve its tensile strength, modulus, and toughness, while

reducing elongation at break. The mechanical properties are influenced by interfacial adhesion and CNT dispersion.

- Graphene nanoplatelets (GNPs): Adding GNPs to PLA can enhance its mechanical properties, depending on factors such as raster direction and nanoplatelet size. Larger GNPs and optimizing raster orientation can improve the mechanical capabilities of graphene-reinforced PLA.
- Short carbon fibers (SCFs): Incorporating SCFs into PLA has been found to enhance its tensile and shear modulus in various printing directions. Continuous carbon fibers can also increase the tensile and flexural behavior of PLA, although they may reduce failure strain.
- Combinations of carbon nanofillers: Using multiple carbon nanofillers, such as GNPs and multi-wall carbon nanotubes (MWCNTs), can produce PLA nanocomposites with better mechanical properties compared to single fillers. For example, adding SCFs and graphene to PLA tripled its mechanical strength [134].

The maximum filler content is typically limited to avoid drastically decreasing the elastic strain of the composites and to allow adequate extrusion of the filaments during FFF/FDM printing. Optimizing printing parameters, such as temperature and infill, can also influence the mechanical properties of PLA nanocomposites.

The addition of carbon nanotubes to polylactic acid (PLA) composites during FDM printing can significantly improve the mechanical, thermal, and electrical properties of the resulting materials. CNTs act as reinforcing agents, increasing the mechanical strength and stiffness of the PLA matrix by providing additional load-bearing capacity and resistance to deformation. This aspect can improve the dimensional accuracy of 3D-printed PLA parts by reducing the warpage and shrinkage that can occur during the printing process. The strong interfacial bonding between CNTs and PLA matrix enhances the mechanical properties of the composite by reducing the likelihood of debonding and improving the transfer of stresses between the CNTs and the matrix. These nanofillers can form a network structure within the PLA matrix, which enhances the mechanical properties of the composite by providing additional mechanical reinforcement and improving the resistance to deformation [135,136].

The CNT content has a significant influence on the PLA/CNT composite, with the optimal CNT loading depending on the specific application and desired properties. The mechanical properties improve by increasing CNT content up to a certain threshold, beyond which the benefits may plateau or even diminish due to issues like CNT agglomeration [137]. Studies comparing CNTs with other reinforcements like cellulose nanocrystals (CNCs) also show that CNTs provide superior improvements in mechanical properties [138].

- Effect of CNT Content on Thermal Properties: The addition of CNTs can improve the thermal conductivity of the PLA matrix, which can lead to improved mechanical properties by reducing thermal gradients and stress concentrations within the composite. The presence of CNTs can accelerate the crystallization of PLA, leading to improved mechanical properties by increasing the degree of crystallinity and reducing the likelihood of defects and imperfections within the matrix. The presence of CNTs and other nanofillers like nanoclay increases the thermal stability and storage modulus of PLA composites, making them more robust at higher temperatures [139].
- Effect of CNT Content on Electrical Properties: The electrical conductivity of PLA/CNT composites has also been investigated, with the addition of CNTs being shown to significantly improve the electrical conductivity of the materials. The CNT content has a significant influence on the electrical properties of PLA/CNT composites during FDM printing. The electrical resistivity varied from approximately $1 \times 10^{12} \Omega/\text{m}^2$ to $1 \times 10^2 \Omega/\text{m}^2$ for CNT contents ranging from 0 wt. % to 8 wt. % [139].

- Effect of CNT on the mechanical properties: The optimal carbon nanotube (CNT) content for achieving the best mechanical properties in PLA/CNT composites is still a topic of ongoing research. However, studies have shown that a CNT content of around 5–10 wt. % can result in significant improvements in mechanical properties (10–60% in tensile strength, up to 30% for flexural strength) compared to neat PLA [140]. It has been found that a 6% CNT content led to a substantial increase in tensile and flexural strength, as well as improved electrical conductivity [139]. However, in other studies, it has been found that while CNT inclusion increased the Young's modulus by 30% at 5% CNT loading, it reduced tensile strength and overall toughness [137].

CNT structure, as well as the FDM process parameters such as extrusion temperature, building direction, infill percentage and geometry, and layer height were key factors in determining the properties of the printed materials [33].

- CNT structure and dimensions: The type (single-walled carbon nanotubes, SWCNTs, multi-walled carbon nanotubes, MWCNTs) and length of CNTs play crucial roles in determining the performance of 3D-printed parts. Longer carbon nanotubes (typically 0.65–1.3 mm) result in higher thermal and electrical conductivities, but no appreciable change in the mechanical properties of PLA/CNT composites during FDM printing [141]. SWCNTs have a more significant impact on the material properties than MWCNTs, but they are generally more expensive. Long MWCNT inclusion determines better performance at lower concentrations [142].
- Nozzle temperature: The optimal printing temperature range for PLA-CNT composites is between 180 °C and 220 °C, with an optimal printing temperature of around 200 °C for tensile strength and 220 °C for flexural strength. A higher printing temperature can lead to improved bonding between the PLA matrix and CNTs, resulting in improved mechanical properties, but may also reduce the impact strength of the composite material [143]. Higher extrusion temperatures can reduce the void fraction in the printed parts but may also result in less alignment of CNTs due to radial flow and fusion between adjacent layers [137]. For better electrical and thermal conductivity, a lower temperature of 200 °C is preferred [139].
- Layer height and infill geometry: The specimens printed at 0.100 mm layer height, gyroid-type infill geometry and number of perimeters of 6 have maximum tensile strength [144]. For better thermal and electrical conductivity, greater layer heights are more desirable [139].
- Build direction: The mechanical properties of 3D-printed PLA composites exhibit significant anisotropy based on build orientation. Tensile strength and Young's modulus are higher when the material is printed in a flat orientation compared to an upright orientation [93].

Functionalized MWCNTs can significantly enhance the mechanical properties of polymer composites. The functionalization of carbon nanotubes (CNTs) through mild acid treatment enhances their nucleating effect during polylactic acid (PLA) crystallization and promotes better dispersion of the CNTs within the PLA matrix. The PLA/f-CNT nanocomposite exhibits higher degrees of crystallinity, as expected, because f-CNTs act more efficiently as nucleating agents than c-CNTs.

Differential Scanning Calorimetry (DSC) analysis revealed no thermal property gradients in 3D-printed specimens across all analyzed samples, including pure PLA, PLA/c-CNT, and PLA/f-CNT. This uniformity in thermal properties, encompassing transition temperatures and degrees of crystallinity, was consistent across the top, central, and base layers of the printed specimens. Furthermore, the 3D printing process did not alter the melting temperature of the materials, indicating that the thermal stability of the composites

remained unaffected. The surface functionalization of carbon nanotubes (CNTs) significantly improved the composite's mechanical performance. Specifically, the PLA/f-CNT samples exhibited a 43% higher storage modulus at body temperature (37 °C) compared to PLA/c-CNT samples, indicating that functionalized CNTs act as more effective reinforcing agents. Scanning Electron Microscopy (SEM) imaging of the fracture interfaces further revealed enhanced interlayer adhesion in PLA/f-CNT samples (Figure 8). This improvement is attributed to the better dispersion of functionalized CNTs within the PLA matrix, resulting in a more uniform material flow during the printing process. Under tensile stress, PLA/f-CNT samples demonstrated markedly superior mechanical properties, with layer-to-layer adhesion contributing to a significant increase in tensile strength (from 29.4 ± 0.7 MPa in PLA/c-CNT to 41.6 ± 1.4 MPa in PLA/f-CNT). These findings highlight the efficacy of CNT surface modification in enhancing the thermal and mechanical properties of 3D-printed PLA/CNT nanocomposites. In particular, the study underscores the role of mild acid treatment (HNO_3 , 5 mol L^{-1}) in functionalizing CNTs and optimizing their reinforcing potential [145].

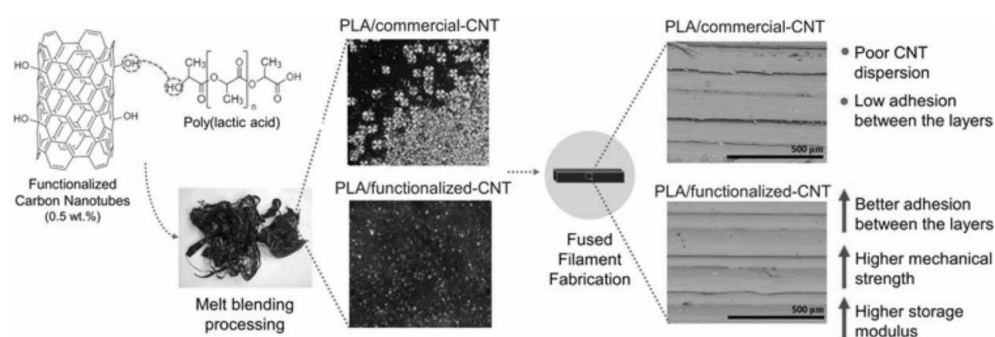


Figure 8. Differences between PLA/commercial-CNT and PLA/functionalized-CNT [reproduced with permission from [145].

2.4. Natural and Synthetic Polymer Blends with Biomass Fillers

2.4.1. Hydroxypropyl-Methylcellulose-Reinforced PLA

Biocompatible hydroxypropyl methylcellulose (HPMC)/polylactic acid (PLA) composites were successfully fabricated as filaments and 3D-printed parts using fused deposition modeling (FDM). This study examined the effects of HPMC content on various properties, including microstructure, chemical structure, thermal behavior, mechanical performance, and water contact angle (CA). The results demonstrated a uniform distribution and dispersion of HPMC within the PLA matrix. Incorporating HPMC up to a concentration of 7% did not affect the chemical structure of PLA during the melt blending and filament extrusion processes. However, HPMC incorporation significantly influenced the thermal properties of the composites, leading to an increased glass transition temperature and a reduced cold crystallization temperature [146]. While the tensile strengths of the composite filaments were comparable to those of neat PLA, the tensile and impact strengths of the 3D-printed samples decreased as the HPMC content increased. This reduction was attributed to increased porosity induced by the presence of HPMC. Additionally, the incorporation of HPMC resulted in a lower water contact angle, which indicates enhanced hydrophilicity. This characteristic could be particularly advantageous for applications in the biomedical field, where surface wettability plays a critical role.

2.4.2. PLA with Lignin and Polymerized-Lignin-Treated NFC

Composite PLA filaments containing unmodified and lignin/polymerized lignin surface-modified nanofibrillated cellulose (NFC) were analyzed to assess their mechanical, thermal, and structural properties. The addition of NFC was found to reduce the stretch-

bility, toughness, breaking tenacity, bending stiffness, and compression resistance of the filaments, while slightly enhancing their initial modulus. Despite a marginal toughening effect imparted by NFC, the improvement was limited due to poor interfacial interactions between NFC and the PLA matrix [147].

The mechanical performance of the composite filaments was closely associated with the NFC's surface modification and concentration within the PLA matrix. When the NFC content was increased to 5 wt. %, the mechanical properties showed the most significant deterioration. However, incorporating lignin/polymerized lignin surface-modified NFC mitigated the decline in mechanical properties and resulted in an increase in storage modulus. The observed limitations in toughness improvement were attributed to poor interfacial adhesion and the presence of NFC agglomerates. These agglomerates, characterized by irregular plate-like shapes and uneven dispersion, acted as structural weak points, thereby impairing the mechanical integrity of the filaments. Scanning Electron Microscopy (SEM) images revealed the structural inconsistencies, while Fourier Transform Infrared (FTIR) analysis confirmed interactions between lignin-modified NFC and the PLA matrix. Dynamic Mechanical Analysis (DMA) further demonstrated a notable increase in elasticity with the addition of modified NFC. Although no significant differences in thermal stability were observed between filaments containing unmodified and modified NFC, the composite filaments exhibited an enhanced crystallization rate compared to neat PLA [148].

Despite only minor variations in mechanical properties, the incorporation of NFC improved the thermal stability of the composites. Lignin, known for its antioxidant properties and UV protection capability, enhanced the thermal oxidative resistance of the filaments, thereby extending the lifespan of 3D-printed objects. Additionally, the light-brown and dark-brown hues imparted by lignin/polymerized lignin surface-modified NFC conferred a unique and aesthetically appealing appearance to the filaments and their corresponding 3D-printed constructs [149].

2.4.3. PLA with Acetylated Tannin

This study investigated the properties and 3D printability of a composite material composed of Polylactic Acid (PLA) and Acetylated Tannin (AT). The acetylation of tannin enhanced its dispersion within the PLA matrix, enabling the successful fabrication of PLA/AT composite filaments using a twin-screw extrusion process. The inclusion of 20 wt. % AT in the PLA matrix did not significantly compromise the tensile properties of the composite. Thermogravimetric analysis indicated that the PLA/AT composites could be safely processed at 3D printing temperatures below 250 °C to avoid thermal decomposition. While acetylated tannin improved the overall printability of PLA systems, optimal printability was achieved at temperatures below 220 °C to prevent phase separation and aggregation of AT, especially at higher loading levels [150].

The incorporation of acetylated tannin at varying concentrations did not substantially affect the melting and glass transition temperatures of PLA, as it had minimal impact on the intermolecular interactions or chain flexibility of the PLA polymer. However, a reduction in the crystallinity of PLA/AT composites was observed, which accelerated their degradation in aquatic environments, particularly under alkaline conditions. This accelerated degradation could be advantageous for short-term biomedical applications, such as implantable devices, where controlled degradation is a desirable attribute [151].

2.4.4. PLA with Cork

Biodegradable composites were synthesized, composed of cork and Polylactic Acid (PLA) with varying proportions of cork. A decline was observed in the tensile mechanical attributes of the composites as the proportion of cork was augmented. The impact resistance

demonstrated an initial decrease with the incorporation of cork; however, it exhibited an increase with further escalation in the cork content. The viscoelastic characteristics of the composites displayed a diminishing trend with the increase in cork content. In contrast, the specific modulus and specific strength of the composites increased with higher cork content, highlighting the potential of cork–PLA composites for lightweight and impact-resistant 3D-printed structures. This improvement in specific mechanical properties underscores their suitability for advanced engineering applications. A filament composed of a 5% *w/w* cork–PLA composite was successfully developed, demonstrating compatibility with fused deposition modeling (FDM) processes. The 3D-printed cork–PLA composite exhibited slightly reduced tensile mechanical properties compared to its compression-molded counterpart. However, an exception was observed in elongation at break, where the 3D-printed composite displayed superior ductility, emphasizing its potential for applications requiring enhanced flexibility and resilience [152].

2.4.5. PLA/Wood Flour

Composite filaments of Wood Fiber (WF) and Polylactic Acid (PLA) were synthesized, and their properties were evaluated in this study. Additionally, 3D specimens were fabricated utilizing the Fused Deposition Modelling (FDM) technique. The study tells us that WF/PLA composite filament demonstrated compatibility with the FDM process, indicating its suitability for 3D printing. Moreover, the incorporation of WF resulted in alterations in the microstructure of the PLA fracture surface. The interfaces between the WF and PLA were distinctly visible and the resistance to initial deformation of the composite was observed to be enhanced upon the addition of WF, in comparison to pure PLA. Also, the onset temperature for thermal degradation of the composites exhibited a slight decrease, while the final residual ratio post-thermal decomposition of the composites showed an increase and the addition of WF at a concentration of 5 wt. % did not influence the melting temperature of the PLA. [153]

Parameters of 0.2 mm layer height, 0.7 mm nozzle diameter, 75% fill density, and 35 mm/s velocity maximize the flexural strength of wood–PLA composite parts built through FFF. [154]

2.4.6. PLA/HA with PCL Addition

The fabrication of bespoke materials, composed of biocompatible and biodegradable polymers either independently or in conjunction with mineral components, resulted in printable substances possessing chemical stability and mechanical attributes conducive to bone regeneration. The mechanical characteristics were validated to meet the mechanical threshold requisite for trabecular bone applications. The tailoring of degradation rates exhibited a strong correlation with the material composition, indicating an enhancement through the integration of mineral phases, such as hydroxyapatite, which further accelerated the degradation of PLA–PCL amalgamations. This, in conjunction with the introduction of regulated porosity and scaffold architecture, could potentially facilitate the control and equilibrium of biomaterial resorption and neo-osteogenesis as required [155].

2.4.7. PLA with TPS and ESO

This research is driven by the current market demand for cost-effective alternatives to Polylactic Acid (PLA). In this study, novel compositions based on PLA, modified by Thermoplastic Starch (TPS) and Epoxidized Soybean Oil (ESO), were developed to enhance the ductility of PLA and reduce the cost of the products without compromising their biodegradability [156]. The efficacy of the proposed compositions was validated by studying their rheological, mechanical, and thermal properties, water resistance, and compostability. An increase in the Melt Flow Rate (MFR) value resulted in enhanced

adaptability to injection and blow molding processes, thereby expanding the range of short-life application products from a technological perspective. To evaluate the suitability of the obtained PLA/TPS (thermoplastic starch) blends for various packaging industry applications, their mechanical properties were thoroughly analyzed. The incorporation of epoxidized soybean oil (ESO) resulted in materials with enhanced softness, improved impact strength (up to 16.69 kJ/m²), and increased tensile and ductile properties, including an elongation at break of approximately 8.8%, compared to native PLA. Scanning Electron Microscopy (SEM) of fractured surfaces confirmed these improvements. Additionally, the presence of ESO in the blends was observed to delay water diffusion into the matrix, thereby potentially improving the dimensional stability of products subjected to short-term water exposure. The modified TPS, prepared with ESO, was shown to be processable using standard PLA machinery, facilitating its integration into existing production systems. Furthermore, the ability to substitute up to 25% of PLA with ESO-modified TPS offers a cost-effective alternative while maintaining comparable properties and compostability to that of pure PLA, underscoring its potential as a sustainable material for packaging applications [157].

Several other studies involving the usage of different fillers and PLA for 3D printing applications are summarized in Table 3.

Table 3. Composite filaments and 3D-printed materials involving PLA and various natural and synthetic fillers.

Type	Reinforcement/Additive	Description	Properties	Applications	Reference
Particle and fiber hybrid-reinforced PLA	MXene (Ti ₃ C ₂ T _x) and recycled carbon fiber (rCF)	MrCF (fiber mass fraction 10 wt. % with 1 wt. % Ti ₃ C ₂ T _x) and 178 g of dried PLA	Compared to pure PLA, the modified PLA displayed significant improvements: 15.6% in toughness, 112.1% in flexural strength, and 31.8% in notched impact strength.	The modified PLA demonstrated superior electromagnetic shielding performance due to the absorption properties of the composite material.	[158]
Particle-based composite	Ferronickel slag (FNS)	composites with FNS contents of 2.0, 6.0, 10.0, and 14.0 wt. %	PLA/5.0 wt. % FNS composite exhibited the most significant improvement in mechanical properties, with a roughly 18% increase in both tensile and flexural strength compared to unfilled PLA thermoplastic		[159]
	Magnesium	1% Mg reported to PLA	Among the 3D-printed samples with different infill orientations ($\theta = 0^\circ, 45^\circ, \pm 45^\circ, 90^\circ$), the highest UTS was measured in specimens with 0° infill orientation (UTS = 43 MPa), whereas the lowest UTS was measured for the 90° infill orientation (UTS = 26 MPa). Mg particles also reduce the mechanical properties at all infill orientations.		[160]
	Parawood (<i>Hevea brasiliensis</i>)	Four different parawood powder weight ratios were blended with PLA, encompassing 0%, 5%, 10%, and 15% (w/w)	The maximum tensile strength was attained when the parawood powder content was 15% w/w.	Large-scale screw-extrusion 3D printing process for producing furniture parts	[161]

Table 3. Cont.

Type	Reinforcement/Additive	Description	Properties	Applications	Reference
	Pyrolyzed HSC (hazelnut shell carbon)	2 % HSC was added to the PLA matrix	The 3D-printed PLA-HSC parts demonstrated excellent photothermal performance with a light absorption intensity of around 93%	Low-cost, compostable, high-efficiency photothermal conversion materials with shaping freedom	[162]
	Salix alba sawdust	1%, 2%, 3%, and 4% (weight %) Salix alba were loaded in the PLA matrix.		PLA-salix alba-based composite feedstock has the controlled MFI and may be used for scaffold preparation in biomedical applications.	[163]
	PLA/Olive wood waste	olive wood scraps (with an amount ranging between 10 and 20% by weight)	The use of wooden scraps in place of virgin PLA granulate reveals a rise in the impact in the extrusion (ca. 27%) and 3D printing (11%) stages	Environmental benefits resulting from the inclusion of wood scraps in PLA filaments (20% of wood corresponds to 10% environmental impact reduction) supporting further research in this area.	[164]
	Cu ₂ O nanoparticles (50-100 nm diameter)	PLA-3 wt. % Cu ₂ O mixture	Superior mechanical performance of the 3D-printed nanocomposite at a 0° raster angle, while the mechanical properties gradually decreased for raster angles of 45° and 90°.	This composite can be utilized for the fabrication of various prostheses featuring specific groove geometries, bio parts in medical devices, robotics surgical systems, and implants	[165]
	PLA/MgAl ₂ O ₄ :Sm ³⁺ composite filaments	Composite filaments of PLA with different amounts of phosphors (0, 1, 2, 3 and 4 phr)	Luminescence intensity of the composites regularly increased with the inorganic phosphor contents	Luminescent bioplastic composite filaments. Filaments and samples of the composites emitted pink-orange light under UV light	[166]
Sheet composite	graphene oxide (GO)	different content of GO (0.4, 0.8, 1.6, 2.4 and 4.0 wt. %) reported to PLA	PLA/GO scrolled fibers and printed fibers with graphene content of 0.4 wt. % exhibit outstanding mechanical properties with strength increases of about 32.7% and 35.2%.		[167]
Polymer-based composite	PLA-TPU	50%, 70% and 90% TPU reported to PLA	The UTS values for PLA50, PLA70, and PLA90 were achieved at 27.27 MPa, 40.91 MPa, and 54.18 MPa, respectively. Also, the fracture toughness results were consistent with the mechanical properties. The PLA90 had 1.69 and 2.36 times higher fracture toughness than the PLA70 and PLA50 compounds, respectively.	By increasing the amount of TPU, the printability decreased due to higher melt strength and viscosity, incomplete melting, feeding problems caused by buckling, and incomplete integration between adjacent rasters and layers.	[168]

Table 3. Cont.

Type	Reinforcement/Additive	Description	Properties	Applications	Reference
	thermoplastic starch (TPS)/poly(lactic acid) (PLA)/poly(butylene adipate-co-terephthalate) (PBAT) composite	Ratio of TPS:PLA:PBAT was fixed at 50:40:10 wt. %.	113% increase in elongation at break and the 190% rise in impact strength compared to PLA	highly renewable filaments for 3D printing	[169]
	PLA with biodegradable elastomer poly(butylene adipate-co-terephthalate) (PBAT) and poly(methyl methacrylate) (PMMA)		Tensile strength and breaking elongation were 94.8% and 3650%, respectively, of that of 3D-printed pure SC-PLA	Controlled compatibilization effect of PMMA endows PBAT with good dispersibility in the quaternary system, without affecting the hierarchical crystallization of enantiomeric PLA matrices for complete stereo-complexation	[170]
	Chitosan	PLA and 10 wt. % chitosan	The acidic environment caused by the degradation of PLA can be counteracted by chitosan, probably due to its protonation.	Biocomposite materials	[171]

3. Conclusions

In the dynamic landscape of additive manufacturing, the quest for high-performance materials continues, and our exploration of reinforced PLA composites has revealed promising innovations and practical applications. The integration of natural fibers into PLA enhances strength and stiffness, offering an eco-friendly alternative while maintaining mechanical integrity. By incorporating metallic particles, researchers have pushed the boundaries of PLA's capabilities, improving thermal and electrical properties and expanding their utility in functional parts. PLA composites reinforced with cellulose fibers demonstrate excellent printability and mechanical performance, with the synergy between PLA and cellulose opening doors to sustainable materials for various industries. Carbon fibers provide significant improvements in tensile strength, sometimes exceeding a 100% increase when loaded at 15%, though these materials require careful handling to prevent clogging and ensure uniform dispersion. Glass fibers enhance flexural strength and thermal stability but tend to make composites brittle, reducing impact resistance. Natural fibers, such as kenaf and hemp, improve sustainability and weight reduction but are limited by moisture absorption and mechanical stability, which can affect layer adhesion. Among particle reinforcements, calcium carbonate improves stiffness, dimensional stability, and printability, though large particles can cause agglomeration and reduce mechanical performance if not properly managed. Carbon nanotubes (CNTs) show potential in improving mechanical, thermal, and electrical properties, though their effectiveness depends on proper dispersion and bonding within the PLA, with surface treatments enhancing their effects. However, challenges like clogging, dispersion issues, and moisture absorption remain common for both synthetic and natural fibers in FDM printing, requiring adjustments in nozzle size, temperature, and other parameters to facilitate smoother flow. Continuous carbon fiber composites stand out for high-strength applications but require specialized equipment and processing, while natural fibers align with eco-friendly goals but underperform compared with synthetic fibers like carbon and glass, which offer superior properties. Among particle-based systems, calcium carbonate is particularly promising for improving mechanical properties and printability without significant processing challenges. Suit-

able printing parameters, including higher temperatures (230–250 °C) for particles, lower temperatures (below 220 °C) for natural fibers, increased infill density (50–70 %), slower printing speeds (10–20 mm/s), and lower layer heights (0.1–0.2 mm), are critical for maximizing performance, particularly in fiber-reinforced composites. While each reinforcement system presents unique benefits and challenges, continuous carbon fibers and calcium carbonate-based composites appear to offer the most promising results depending on the application. The optimization of printing parameters, such as nozzle size, temperature, layer height, and infill density, is crucial for achieving the best outcomes. Reinforced PLA composites align with global efforts to reduce reliance on fossil-based polymers, and the journey toward optimized PLA composites involves collaboration across disciplines, including materials science, engineering, and design. By bridging the gap between theory and practice, reinforced PLA composites hold immense promise for a greener, more resilient additive manufacturing industry.

Funding: This research received no external funding.

Conflicts of Interest: The authors declare no conflict of interest.

Abbreviations

PLA	polylactic acid
FDM	fused deposition modeling
ABS	poly (acrylonitrile-co-butadiene-co-styrene)
PETG	polyethylene-terephthalate glycol
FFF	fused filament fabrication
PHB	polyhydroxy butyrate
PBS	polybutylene succinate
CPA-PLA	carbon fiber-reinforced polylactic acid
GFs	glass fiber
OG	octylgallate
LG	lauryl gallate
PALF	pineapple leaf fiber
FTIR	Fourier transform infrared
XRD	X-ray diffraction
HBICP	hardwood bleached kraft pulp
LCNF	lignocellulose nanofiber
SGFs	Short glass fibers
LS	limestone
WES	white eggshell
BSA-FITC	Bovine serum albumin -fluorescein isothiocyanate
S/O/W	solvent/oil/water
DCM	dichloro methane
UTS	Ultimate tensile strength
BN	Boron nitride
SCFs	short carbon fibers
MWCNTs	Multiwalled carbon nanotubes
SEM	scanning electron microscopy
AT	acetylated tannin
DMA	dynamic mechanical analysis
PCL	polycaprolactone
ESO	Epoxidized soybean oil

TPS	Thermoplastic starch
MFR	Melt flow rate
FNS	Ferronickel slab
PBAT	polybutylene adipate-co-terephthalate
PMMA	poly(methyl methacrylate)
f-CNTs	functionalized carbon nanotubes
phr	parts per hundred resin (polymer)

References

- Hottle, T.; Bilec, M.; Landis, A. Sustainability assessments of bio-based polymers. *Polym. Degrad. Stab.* **2013**, *98*, 1898–1907. [[CrossRef](#)]
- Li, G.; Zhao, M.; Xu, F.; Yang, B.; Li, X.; Meng, X.; Teng, L.; Sun, F.; Li, Y. Synthesis and Biological Application of Polylactic Acid. *Molecules* **2020**, *25*, 5023. [[CrossRef](#)] [[PubMed](#)]
- Caminero, M.; Chacón, J.; García-Plaza, E.; Núñez, P.; Reverte, J.; Bécar, J. Additive Manufacturing of PLA-Based Composites Using Fused Filament Fabrication: Effect of Graphene Nanoplatelet Reinforcement on Mechanical Properties, Dimensional Accuracy and Texture. *Polymers* **2019**, *11*, 799. [[CrossRef](#)] [[PubMed](#)]
- Kaczmarek, H.; Nowicki, M.; Vuković-Kwiatkowska, I.; Nowakowska, S. Crosslinked blends of poly (lactic acid) and polyacrylates: AFM, DSC and XRD studies. *J. Polym. Res.* **2013**, *20*, 91. [[CrossRef](#)]
- Ilyas, R.A.; Sapuan, S.M.; Harussani, M.M.; Hakimi, M.Y.A.Y.; Haziq, M.Z.M.; Atikah, M.S.N.; Asyraf, M.R.M.; Ishak, M.R.; Razman, M.R.; Nurazzi, N.M.; et al. Polylactic Acid (PLA) Biocomposite: Processing, Additive Manufacturing and Advanced Applications. *Polymers* **2021**, *13*, 1326. [[CrossRef](#)]
- Ncube, L.K.; Ude, A.U.; Ogunmuyiwa, E.N.; Zulkifli, R.; Beas, I.N. Environmental Impact of Food Packaging Materials: A Review of Contemporary Development from Conventional Plastics to Polylactic Acid Based Materials. *Materials* **2020**, *13*, 4994. [[CrossRef](#)]
- Gu, J.; Wensing, M.; Uhde, E.; Salthammer, T. Characterization of particulate and gaseous pollutants emitted during operation of a desktop 3D printer. *Environ. Int.* **2019**, *123*, 476–485. [[CrossRef](#)]
- Potter, P.M.; Al-Abed, S.R.; Hasan, F.; Lomnicki, S.M. Influence of polymer additives on gas-phase emissions from 3D printer filaments. *Chemosphere* **2021**, *279*, 130543. [[CrossRef](#)]
- Alberts, E.; Ballentine, M.; Barnes, E.; Kennedy, A. Impact of metal additives on particle emission profiles from a fused filament fabrication 3D printer. *Atmos. Environ.* **2021**, *244*, 117956. [[CrossRef](#)]
- Bhagia, S.; Bornani, K.; Agrawal, R.; Satlewal, A.; Đurković, J.; Lagaña, R.; Bhagia, M.; Yoo, C.G.; Zhao, X.; Kunc, V.; et al. Critical review of FDM 3D printing of PLA biocomposites filled with biomass resources, characterization, biodegradability, upcycling and opportunities for biorefineries. *Appl. Mater. Today* **2021**, *24*, 101078. [[CrossRef](#)]
- Cojocar, V.; Frunzaverde, D.; Miclosina, C.-O.; Marginean, G. The Influence of the Process Parameters on the Mechanical Properties of PLA Specimens Produced by Fused Filament Fabrication—A Review. *Polymers* **2022**, *14*, 886. [[CrossRef](#)] [[PubMed](#)]
- Weber, R.; Zhang, Q.; Wong, J.; Davis, A.; Black, M. Fine particulate and chemical emissions from desktop 3D printers. *NIP Digit. Fabr. Conf.* **2016**, *32*, 121–123. [[CrossRef](#)]
- Thumsorn, S.; Prasong, W.; Kurose, T.; Ishigami, A.; Kobayashi, Y.; Ito, H. Rheological Behavior and Dynamic Mechanical Properties for Interpretation of Layer Adhesion in FDM 3D Printing. *Polymers* **2022**, *14*, 2721. [[CrossRef](#)]
- Rodríguez-Panes, A.; Claver, J.; Camacho, A.M. The Influence of Manufacturing Parameters on the Mechanical Behaviour of PLA and ABS Pieces Manufactured by FDM: A Comparative Analysis. *Materials* **2018**, *11*, 1333. [[CrossRef](#)] [[PubMed](#)]
- Tao, Y.; Li, P.; Zhang, J.; Wang, S.; Shi, S.Q.; Kong, F. A review of fused filament fabrication of continuous natural fiber reinforced thermoplastic composites: Techniques and materials. *Polym. Compos.* **2023**, *44*, 8200–8222. [[CrossRef](#)]
- Błędzki, A.; Gassan, J. Composites reinforced with cellulose based fibres. *Prog. Polym. Sci.* **1999**, *24*, 221–274. [[CrossRef](#)]
- Yusri, M.A.H.M.; Zuhri, M.Y.M.; Ishak, M.R.; Azman, M.A. The Capabilities of Honeycomb Core Structures Made of Kenaf/Polylactic Acid Composite under Compression Loading. *Polymers* **2023**, *15*, 2179. [[CrossRef](#)]
- Brząkalski, D.; Sztorch, B.; Frydrych, M.; Pakuła, D.; Dydek, K.; Kozera, R.; Boczowska, A.; Marciniak, B.; Przekop, R.E. Limonene Derivative of Spherosilicate as a Polylactide Modifier for Applications in 3D Printing Technology. *Molecules* **2020**, *25*, 5882. [[CrossRef](#)]
- Buj-Corral, I.; Sivatte-Adroer, M. An Experimental Investigation about the Dimensional Accuracy and the Porosity of Copper-Filled PLA Fused Filament Fabrication Parts. *Metals* **2023**, *13*, 1608. [[CrossRef](#)]
- Sztorch, B.; Brząkalski, D.; Pakuła, D.; Frydrych, M.; Špitalský, Z.; Przekop, R.E. Natural and Synthetic Polymer Fillers for Applications in 3D Printing—FDM Technology Area. *Solids* **2022**, *3*, 508–548. [[CrossRef](#)]
- Kantaros, A.; Soulis, E.; Petrescu, F.I.T.; Ganetsos, T. Advanced Composite Materials Utilized in FDM/FFF 3D Printing Manufacturing Processes: The Case of Filled Filaments. *Materials* **2023**, *16*, 6210. [[CrossRef](#)] [[PubMed](#)]

22. Fernández, V.; García, A.; Camacho, A.M.; Claver, J.; Rodríguez, A.; Sebastián, M.A. Methodology to estimate the modulus of elasticity of parts manufactured by FFF/FDM combining finite element simulations and experimental tests. *IOP Conf. Ser. Mater. Sci. Eng.* **2021**, *1193*, 012103. [[CrossRef](#)]
23. Anwajler, B.; Zdybel, E.; Tomaszewska-Ciosk, E. Innovative Polymer Composites with Natural Fillers Produced by Additive Manufacturing (3D Printing)—A Literature Review. *Polymers* **2023**, *15*, 3534. [[CrossRef](#)] [[PubMed](#)]
24. Pal, A.K.; Mohanty, A.K.; Misra, M. Additive manufacturing technology of polymeric materials for customized products: Recent developments and future prospective. *RSC Adv.* **2021**, *11*, 36398–36438. [[CrossRef](#)]
25. Rafiee, R.; Amini, M.; Zehtabzadeh, H. Examining Tensile Properties in Nanocomposite Samples Fabricated Through Extrusion-Based Additive Manufacturing. *Arab. J. Sci. Eng.* **2023**, *49*, 10913–10926. [[CrossRef](#)]
26. Ryan, K.; Down, M.; Hurst, N.; Keefe, E.; Banks, C. Additive manufacturing (3D printing) of electrically conductive polymers and polymer nanocomposites and their applications. *eScience* **2022**, *2*, 365–381. [[CrossRef](#)]
27. Hu, C.; Hau, W.N.J.; Chen, W.; Qin, Q.-H. The fabrication of long carbon fiber reinforced polylactic acid composites via fused deposition modelling: Experimental analysis and machine learning. *J. Compos. Mater.* **2021**, *55*, 1459–1472. [[CrossRef](#)]
28. Do, T.; Le, M.; Nguyen, T.; Le Thai, H. Effect of Infill Density and Printing Patterns on Compressive Strength of ABS, PLA, PLA-CF Materials for FDM 3D Printing. *Mater. Sci. Forum* **2022**, *1068*, 19–27. [[CrossRef](#)]
29. Valvez, S.; Santos, P.; Parente, J.M.; Silva, M.P.; Reis, P.N.B. 3D printed continuous carbon fiber reinforced PLA composites: A short review. *Procedia Struct. Integr.* **2020**, *25*, 394–399. [[CrossRef](#)]
30. Cao, M.; Cui, T.; Yue, Y.; Li, C.; Guo, X.; Jia, X.; Wang, B. Investigation of Carbon Fiber on the Tensile Property of FDM-Produced PLA Specimen. *Polymers* **2022**, *14*, 5230. [[CrossRef](#)]
31. Shah, A.K.; Jain, A. Microstructure and mechanical properties of filament and fused deposition modelling printed polylactic-acid and carbon-fiber reinforced polylactic-acid. *J. Reinf. Plast. Compos.* **2024**, *43*, 516–531. [[CrossRef](#)]
32. Dou, H.; Cheng, Y.; Ye, W.; Zhang, D.; Li, J.; Miao, Z.; Rudykh, S. Effect of Process Parameters on Tensile Mechanical Properties of 3D Printing Continuous Carbon Fiber-Reinforced PLA Composites. *Materials* **2020**, *13*, 3850. [[CrossRef](#)] [[PubMed](#)]
33. Kamaal, M.; Anas, M.; Rastogi, H.; Bhardwaj, N.; Rahaman, A. Effect of FDM process parameters on mechanical properties of 3D-printed carbon fibre–PLA composite. *Prog. Addit. Manuf.* **2021**, *6*, 63–69. [[CrossRef](#)]
34. Hu, Y.; Ladani, R.B.; Brandt, M.; Li, Y.; Mouritz, A.P. Carbon fibre damage during 3D printing of polymer matrix laminates using the FDM process. *Mater. Des.* **2021**, *205*, 109679. [[CrossRef](#)]
35. Papon, E.A.; Haque, A. Tensile properties, void contents, dispersion and fracture behaviour of 3D printed carbon nanofiber reinforced composites. *J. Reinf. Plast. Compos.* **2018**, *37*, 381–395. [[CrossRef](#)]
36. Papon, E.A.; Haque, A. Fracture toughness of additively manufactured carbon fiber reinforced composites. *Addit. Manuf.* **2019**, *26*, 41–52. [[CrossRef](#)]
37. Krajangsawasdi, N.; Blok, L.G.; Hamerton, I.; Longana, M.L.; Woods, B.K.S.; Ivanov, D.S. Fused Deposition Modelling of Fibre Reinforced Polymer Composites: A Parametric Review. *J. Compos. Sci.* **2021**, *5*, 29. [[CrossRef](#)]
38. Lee, D.; Wu, G.-Y. Parameters Affecting the Mechanical Properties of Three-Dimensional (3D) Printed Carbon Fiber-Reinforced Polylactide Composites. *Polymers* **2020**, *12*, 2456. [[CrossRef](#)]
39. Selvam, A.; Mayilswamy, S.; Whenish, R.; Velu, R.; Subramanian, B. Preparation and Evaluation of the Tensile Characteristics of Carbon Fiber Rod Reinforced 3D Printed Thermoplastic Composites. *J. Compos. Sci.* **2021**, *5*, 8. [[CrossRef](#)]
40. Peng, X.; Zhang, M.; Guo, Z.; Sang, L.; Hou, W. Investigation of processing parameters on tensile performance for FDM-printed carbon fiber reinforced polyamide 6 composites. *Compos. Commun.* **2020**, *22*, 100478. [[CrossRef](#)]
41. Magri, A.E.; El Mabrouk, K.; Vaudreuil, S.; Touhami, M.E. Mechanical properties of CF-reinforced PLA parts manufactured by fused deposition modeling. *J. Thermoplast. Compos. Mater.* **2021**, *34*, 581–595. [[CrossRef](#)]
42. Rao, V.D.P.; Rajiv, P.; Geethika, V.N. Effect of fused deposition modelling (FDM) process parameters on tensile strength of carbon fibre PLA. *Mater. Today Proc.* **2019**, *18 Pt 6*, 2012–2018. [[CrossRef](#)]
43. Öteyaka, M.; Aybar, K.; Öteyaka, H.C. Effect of Infill Ratio on the Tensile and Flexural Properties of Unreinforced and Carbon Fiber-Reinforced Polylactic Acid Manufactured by Fused Deposition Modeling. *J. Mater. Eng. Perform.* **2021**, *30*, 5203–5215. [[CrossRef](#)]
44. Liu, Z.; Lei, Q.; Xing, S. Mechanical characteristics of wood, ceramic, metal and carbon fiber-based PLA composites fabricated by FDM. *J. Mater. Res. Technol.* **2019**, *8*, 3741–3751. [[CrossRef](#)]
45. Chen, K.; Yu, L.; Cui, Y.; Jia, M.; Pan, K. Optimization of printing parameters of 3D-printed continuous glass fiber reinforced polylactic acid composites. *Thin-Walled Struct.* **2021**, *164*, 107717. [[CrossRef](#)]
46. Vinyas, M.; Athul, S.; Harursampath, D.; Thoi, T.N. Experimental evaluation of the mechanical and thermal properties of 3-D printed PLA and its composites. *Mater. Res. Express* **2019**, *6*, 115301. [[CrossRef](#)]
47. Ismail, K.I.; Pang, R.; Ahmed, R.; Yap, T.C. Tensile Properties of In Situ 3D Printed Glass Fiber-Reinforced PLA. *Polymers* **2023**, *15*, 3436. [[CrossRef](#)]

48. Dickson, A.N.; Barry, J.N.; McDonnell, K.A.; Dowling, D.P. Dowling, Fabrication of continuous carbon, glass and Kevlar fibre reinforced polymer composites using additive manufacturing. *Addit. Manuf.* **2017**, *16*, 146–152. [[CrossRef](#)]
49. Arai, S.; Tsunoda, S.; Yamaguchi, A.; Ougizawa, T. Effects of short-glass-fiber content on material and part properties of poly(butylene terephthalate) processed by selective laser sintering. *Addit. Manuf.* **2018**, *21*, 683–693. [[CrossRef](#)]
50. Wang, G.; Zhang, D.; Li, B.; Wan, G.; Zhao, G.; Zhang, A. Strong and thermal-resistance glass fiber-reinforced polylactic acid (PLA) composites enabled by heat treatment. *Int. J. Biol. Macromol.* **2019**, *129*, 448–459. [[CrossRef](#)]
51. Chicos, L.-A.; Pop, M.A.; Zaharia, S.-M.; Lancea, C.; Buican, G.R.; Pascariu, I.S.; Stamate, V.-M. Fused Filament Fabrication of Short Glass Fiber-Reinforced Polylactic Acid Composites: Infill Density Influence on Mechanical and Thermal Properties. *Polymers* **2022**, *14*, 4988. [[CrossRef](#)] [[PubMed](#)]
52. Wang, K.; Chen, Y.; Long, H.; Baghani, M.; Rao, Y.; Peng, Y. Hygrothermal aging effects on the mechanical properties of 3D printed composites with different stacking sequence of continuous glass fiber layers. *Polym. Test.* **2021**, *100*, 107242. [[CrossRef](#)]
53. Varsavas, S.; Kaynak, C. Weathering degradation performance of PLA and its glass fiber reinforced composite. *Mater. Today Commun.* **2017**, *15*, 344–353. [[CrossRef](#)]
54. Wang, G.; Zhang, D.; Wan, G.; Li, B.; Zhao, G. Glass fiber reinforced PLA composite with enhanced mechanical properties, thermal behavior, and foaming ability. *Polymer* **2019**, *181*, 121803. [[CrossRef](#)]
55. Tümer, E.H.; Erbil, H.Y. Extrusion-Based 3D Printing Applications of PLA Composites: A Review. *Coatings* **2021**, *11*, 390. [[CrossRef](#)]
56. Tang, C.; Liu, J.; Yang, Y.; Liu, Y.; Jiang, S.; Hao, W. Effect of process parameters on mechanical properties of 3D printed PLA lattice structures. *Compos. Part C Open Access* **2020**, *3*, 100076. [[CrossRef](#)]
57. Yang, Y.; Yang, B.; Chang, Z.; Duan, J.; Chen, W. Research Status of and Prospects for 3D Printing for Continuous Fiber-Reinforced Thermoplastic Composites. *Polymers* **2023**, *15*, 3653. [[CrossRef](#)]
58. Gunasekaran, K.; Aravinth, V.; Kumaran, C.M.; Madhankumar, K.; Kumar, S.P. Pradeep Kumar, Investigation of mechanical properties of PLA printed materials under varying infill density. *Mater. Today Proc.* **2021**, *45 Pt 2*, 1849–1856. [[CrossRef](#)]
59. Ambati, S.S.; Ambatipudi, R. Effect of infill density and infill pattern on the mechanical properties of 3D printed PLA parts. *Mater. Today Proc.* **2022**, *64 Pt 1*, 804–807. [[CrossRef](#)]
60. Shavandi, A.; Hosseini, S.; Okoro, O.V.; Nie, L.; Babadi, F.E.; Melchels, F. 3D Bioprinting of Lignocellulosic Biomaterials. *Adv. Healthc. Mater.* **2020**, *9*, 2001472. [[CrossRef](#)]
61. Dickson, A.N.; Abourayana, H.M.; Dowling, D.P. 3D Printing of Fibre-Reinforced Thermoplastic Composites Using Fused Filament Fabrication—A Review. *Polymers* **2020**, *12*, 2188. [[CrossRef](#)] [[PubMed](#)]
62. Mazzanti, V.; Malagutti, L.; Mollica, F. FDM 3D Printing of Polymers Containing Natural Fillers: A Review of their Mechanical Properties. *Polymers* **2019**, *11*, 1094. [[CrossRef](#)] [[PubMed](#)]
63. Tarrés, Q.; Melbø, J.; Delgado-Aguilar, M.; Espinach, F.; Mutjé, P.; Chinga-Carrasco, G. Chinga-Carrasco, Bio-polyethylene reinforced with thermomechanical pulp fibers: Mechanical and micromechanical characterization and its application in 3D-printing by fused deposition modelling. *Compos. Part B Eng.* **2018**, *153*, 70–77. [[CrossRef](#)]
64. Le Duigou, A.; Barbé, A.; Guillou, E.; Castro, M. 3D printing of continuous flax fibre reinforced biocomposites for structural applications. *Mater. Des.* **2019**, *180*, 107884. [[CrossRef](#)]
65. Savic, A.; Antonijevic, D.; Jelic, I.; Zakic, D. Thermomechanical behavior of bio-fiber composite thermal insulation panels. *Energy Build.* **2020**, *229*, 110511. [[CrossRef](#)]
66. Asim, M.; Paridah, M.T.; Chandrasekar, M.; Shahroze, R.M.; Jawaid, M.; Nasir, M.; Siakeng, R. Thermal stability of natural fibers and their polymer composites. *Iran. Polym. J.* **2020**, *29*, 625–648. [[CrossRef](#)]
67. Estakhrianhaghighi, E.; Mirabolghasemi, A.; Zhang, Y.; Lessard, L.; Akbarzadeh, A. 3D-Printed Wood-Fiber Reinforced Architected Cellular Composites 2020. *Adv. Eng. Mater.* **2020**, *22*, 2000565. [[CrossRef](#)]
68. Le Duigou, A.; Correa, D.; Ueda, M.; Matsuzaki, R.; Castro, M. A review of 3D and 4D printing of natural fibre biocomposites. *Mater. Des.* **2020**, *194*, 108911. [[CrossRef](#)]
69. Rajendran Royan, N.R.; Leong, J.S.; Chan, W.N.; Tan, J.R.; Shamsuddin, Z.S.B. Current State and Challenges of Natural Fibre-Reinforced Polymer Composites as Feeder in FDM-Based 3D Printing. *Polymers* **2021**, *13*, 2289. [[CrossRef](#)]
70. Parandoush, P.; Lin, D. A review on additive manufacturing of polymer-fiber composites. *Compos. Struct.* **2017**, *182*, 36–53. [[CrossRef](#)]
71. Lee, C.H.; Padzil, F.N.B.M.; Lee, S.H.; Ainun, Z.M.A.; Abdullah, L.C. Potential for Natural Fiber Reinforcement in PLA Polymer Filaments for Fused Deposition Modeling (FDM) Additive Manufacturing: A Review. *Polymers* **2021**, *13*, 1407. [[CrossRef](#)] [[PubMed](#)]
72. Bledzki, A.K.; Jaszkievicz, A.; Scherzer, D. Mechanical properties of PLA composites with man-made cellulose and abaca fibres. *Compos. Part A Appl. Sci. Manuf.* **2009**, *40*, 404–412. [[CrossRef](#)]

73. Rajeshkumar, G.; Seshadri, S.A.; Devnani, G.; Sanjay, M.; Siengchin, S.; Maran, J.P.; Al-Dhabi, N.A.; Karuppiyah, P.; Mariadhas, V.A.; Sivarajasekar, N.; et al. Environment friendly, renewable and sustainable poly lactic acid (PLA) based natural fiber reinforced composites—A comprehensive review. *J. Clean. Prod.* **2021**, *310*, 127483. [CrossRef]
74. Goriparthi, B.K.; Suman, K.N.S.; Rao, N.M. Effect of fiber surface treatments on mechanical and abrasive wear performance of polylactide/jute composites. *Compos. Part A Appl. Sci. Manuf.* **2012**, *43*, 1800–1808. [CrossRef]
75. Vilaseca, F.; Mendez, J.; Pèlach, A.; Llop, M.; Cañigueral, N.; Gironès, J.; Turon, X.; Mutjé, P. Composite materials derived from biodegradable starch polymer and jute strands. *Process Biochem.* **2007**, *42*, 329–334. [CrossRef]
76. Aguado, R.J.; Espinach, F.X.; Julián, F.; Tarrés, Q.; Delgado-Aguilar, M.; Mutjé, P. Tensile Strength of Poly(lactic acid)/Bleached Short Hemp Fiber Fully Green Composites as Replacement for Polypropylene/Glass Fiber. *Polymers* **2023**, *15*, 146. [CrossRef]
77. Deb, D.; Jafferson, J. Natural fibers reinforced FDM 3D printing filaments. *Mater. Today Proc.* **2021**, *46 Pt 2*, 1308–1318. [CrossRef]
78. Filgueira, D.; Holmen, S.; Melbø, J.K.; Moldes, D.; Echtermeyer, A.T.; Chinga-Carrasco, G. Enzymatic-Assisted Modification of Thermomechanical Pulp Fibers To Improve the Interfacial Adhesion with Poly(lactic acid) for 3D Printing. *ACS Sustain. Chem. Eng.* **2017**, *5*, 9338–9346. [CrossRef]
79. Zhang, Q.; Ma, L.; Zhang, X.; Zhang, L.; Wang, Z. Lignocellulose nanofiber/poly(lactic acid) (LCNF/PLA) composite with internal lignin for enhanced performance as 3D printable filament. *Ind. Crops Prod.* **2022**, *178*, 114590. [CrossRef]
80. Ahmed, W.; Alnajjar, F.; Zanelidin, E.; Al-Marzouqi, A.H.; Gochoo, M.; Khalid, S. Implementing FDM 3D Printing Strategies Using Natural Fibers to Produce Biomass Composite. *Materials* **2020**, *13*, 4065. [CrossRef]
81. Billings, C.; Siddique, R.; Sherwood, B.; Hall, J.; Liu, Y. Additive Manufacturing and Characterization of Sustainable Wood Fiber-Reinforced Green Composites. *J. Compos. Sci.* **2023**, *7*, 489. [CrossRef]
82. Shahar, F.S.; Hameed Sultan, M.T.; Safri, S.N.A.; Jawaid, M.; Abu Talib, A.R.; Basri, A.A.; Md Shah, A.U. Physical, thermal and tensile behaviour of 3D printed kenaf/PLA to suggest its usability for ankle-foot orthosis—A preliminary study. *Rapid Prototyp. J.* **2022**, *28*, 1573–1588. [CrossRef]
83. Bajpai, P.K.; Singh, I.; Madaan, J. Tribological behavior of natural fiber reinforced PLA composites. *Wear* **2013**, *297*, 829–840. [CrossRef]
84. Gupta, B.; Revagade, N.; Hilborn, J. Poly(lactic acid) fiber: An overview. *Prog. Polym. Sci.* **2007**, *32*, 455–482. [CrossRef]
85. Mazur, K.E.; Borucka, A.; Kaczor, P.; Gądek, S.; Kuciel, S. Mechanical Performance Under Various Conditions of 3D Printed Polylactide Composites with Natural Fibers. *Preprint* **2021**. Available online: <https://www.researchsquare.com/article/rs-517727/v1> (accessed on 10 December 2024). [CrossRef]
86. Paulo, A.; Santos, J.; da Rocha, J.; Lima, R.; Ribeiro, J. Mechanical Properties of PLA Specimens Obtained by Additive Manufacturing Process Reinforced with Flax Fibers. *J. Compos. Sci.* **2023**, *7*, 27. [CrossRef]
87. Aliotta, L.; Gigante, V.; Coltelli, M.B.; Cinelli, P.; Lazzeri, A. Evaluation of Mechanical and Interfacial Properties of Bio-Composites Based on Poly(Lactic Acid) with Natural Cellulose Fibers. *Int. J. Mol. Sci.* **2019**, *20*, 960. [CrossRef]
88. Graupner, N.; Herrmann, A.S.; Müssig, J. Natural and man-made cellulose fibre-reinforced poly(lactic acid) (PLA) composites: An overview about mechanical characteristics and application areas. *Compos. Part A Appl. Sci. Manuf.* **2009**, *40*, 810–821. [CrossRef]
89. Dogru, A.; Sozen, A.; Neser, G.; Seydibeyoglu, M.O. Effects of Aging and Infill Pattern on Mechanical Properties of Hemp Reinforced PLA Composite Produced by Fused Filament Fabrication (FFF). *Appl. Sci. Eng. Prog.* **2021**, *14*, 651–660. [CrossRef]
90. Yang, T.-C.; Yeh, C.-H. Morphology and Mechanical Properties of 3D Printed Wood Fiber/Poly(lactic acid) Composite Parts Using Fused Deposition Modeling (FDM): The Effects of Printing Speed. *Polymers* **2020**, *12*, 1334. [CrossRef]
91. Gauss, C.; Pickering, K.L.; Graupner, N.; Müssig, J. 3D-printed polylactide composites reinforced with short lyocell fibres—Enhanced mechanical properties based on bio-inspired fibre fibrillation and post-print annealing. *Addit. Manuf.* **2023**, *77*, 103806. [CrossRef]
92. Belarbi, Y.E.; Guessasma, S.; Belhabib, S.; Benmahiddine, F.; Hamami, A.E.A. Effect of Printing Parameters on Mechanical Behaviour of PLA-Flax Printed Structures by Fused Deposition Modelling. *Materials* **2021**, *14*, 5883. [CrossRef] [PubMed]
93. Gonabadi, H.; Yadav, A.; Bull, S.J. The effect of processing parameters on the mechanical characteristics of PLA produced by a 3D FFF printer. *Int. J. Adv. Manuf. Technol.* **2020**, *111*, 695–709. [CrossRef]
94. Mansingh, B.B.; Binoj, J.S.; Tan, Z.Q.; Eugene, W.W.L.; Amornsakchai, T.; Abu Hassan, S.; Goh, K.L. Comprehensive characterization of raw and treated pineapple leaf fiber/poly(lactic acid) green composites manufactured by 3D printing technique. *Polym. Compos.* **2022**, *43*, 6051–6061. [CrossRef]
95. Zhang, Z.; Wang, W.; Li, Y.; Fu, K.; Tong, X.; Cao, B.; Chen, B. 3D printing of cellulose nanofiber/poly(lactic acid) composites via an efficient dispersion method. *Compos. Commun.* **2023**, *43*, 101731. [CrossRef]
96. Inseemesak, B.; Siripaiboon, C.; Somkeattikul, K.; Attasophonwattana, P.; Kiatiwat, T.; Punsuvon, V.; Areeprasert, C. Biocomposite fabrication from pilot-scale steam-exploded coconut fiber and PLA/PBS with mechanical and thermal characterizations. *J. Clean. Prod.* **2022**, *379 Pt 1*, 134517. [CrossRef]
97. Zhao, G.; Liu, H.-Y.; Cui, X.; Du, X.; Zhou, H.; Mai, Y.-W.; Jia, Y.-Y.; Yan, W. Tensile properties of 3D-printed CNT-SGF reinforced PLA composites. *Compos. Sci. Technol.* **2022**, *230 Pt 2*, 109333. [CrossRef]

98. Tenn, N.; Follain, N.; Soulestin, J.; Crétois, R.; Bourbigot, S.; Marais, S. Effect of Nanoclay Hydration on Barrier Properties of PLA/Montmorillonite Based Nanocomposites. *J. Phys. Chem. C* **2012**, *117*, 12117–12135. [[CrossRef](#)]
99. Lenshin, A.S.; Frolova, V.E.; Kannykin, S.V.; Domashevskaya, E.P. Microstructural and Hydrophilic Properties of Polylactide Polymer Samples with Various 3D Printing Patterns. *Polymers* **2024**, *16*, 1281. [[CrossRef](#)]
100. Ghiasi, M.; Abdollahy, M.; Khalesi, M.R.; Ghiasi, E. Control of morphology, specific surface area and agglomeration of precipitated calcium carbonate crystals through a multiphase carbonation process. *CrystEngComm* **2020**, *22*, 1970–1984. [[CrossRef](#)]
101. Faba, S.; Agüero, Á.; Arrieta, M.P.; Martínez, S.; Romero, J.; Torres, A.; Galotto, M.J. Foaming of 3D-Printed PLA/CaCO₃ Composites by Supercritical CO₂ Process for Sustainable Food Contact Materials. *Polymers* **2024**, *16*, 798. [[CrossRef](#)]
102. Varga, P.; Lorinczy, D.; Tóth, L.; Pentek, A.; Nyitrai, M.; Maroti, P. Novel PLA–CaCO₃ composites in additive manufacturing of upper limb casts and orthotics—A feasibility study. *Mater. Res. Express* **2019**, *6*, 045317. [[CrossRef](#)]
103. Donate, R.; Paz, R.; Quintana, Á.; Bordón, P.; Monzón, M. Calcium Carbonate Coating of 3D-Printed PLA Scaffolds Intended for Biomedical Applications. *Polymers* **2023**, *15*, 2506. [[CrossRef](#)] [[PubMed](#)]
104. Zárbynická, L.; Ševčík, R.; Pokorný, J.; Machová, D.; Stránská, E.; Šál, J. CaCO₃ Polymorphs Used as Additives in Filament Production for 3D Printing. *Polymers* **2022**, *14*, 199. [[CrossRef](#)] [[PubMed](#)]
105. Zhu, Y.; Allen, G.; Jones, P.; Adams, J.; Gittins, D.; Heard, P.; Skuse, D. Dispersion characterisation of CaCO₃ particles in PP/CaCO₃ composites. *Compos. Part A Appl. Sci. Manuf.* **2014**, *60*, 38–43. [[CrossRef](#)]
106. Betancourt, N.G.; Cree, D.E. Mechanical Properties of Poly (lactic acid) Composites Reinforced with CaCO₃ Eggshell Based Fillers. *MRS Adv.* **2017**, *2*, 2545–2550. [[CrossRef](#)]
107. Pavon, C.; Aldas, M.; Samper, M.D.; Motoc, D.L.; Ferrandiz, S.; López-Martínez, J. Mechanical, Dynamic-Mechanical, Thermal and Decomposition Behavior of 3D-Printed PLA Reinforced with CaCO₃ Fillers from Natural Resources. *Polymers* **2022**, *14*, 2646. [[CrossRef](#)]
108. Aliotta, L.; Cinelli, P.; Coltelli, M.B.; Lazzeri, A. Rigid filler toughening in PLA-Calcium Carbonate composites: Effect of particle surface treatment and matrix plasticization. *Eur. Polym. J.* **2019**, *113*, 78–88. [[CrossRef](#)]
109. Shi, X.; Zhang, G.; Siligardi, C.; Ori, G.; Lazzeri, A. Comparison of Precipitated Calcium Carbonate/Poly(lactic acid) and Halloysite/Poly(lactic acid) Nanocomposites. *J. Nanomater.* **2015**, *2015*, 905210. [[CrossRef](#)]
110. Zhi, Z.; Liu, R.; Wang, W.; Dewettinck, K.; Bockstaele, F. Recent progress in oil-in-water-in-oil (O/W/O) double emulsions. *Crit. Rev. Food Sci. Nutr.* **2022**, *63*, 6196–6207. [[CrossRef](#)]
111. Kudryavtseva, V.L.; Zhao, L.; Tverdokhlebov, S.I.; Sukhorukov, G.B. Fabrication of PLA/CaCO₃ hybrid micro-particles as carriers for water-soluble bioactive molecules. *Colloids Surf. B Biointerfaces* **2017**, *157*, 481–489. [[CrossRef](#)]
112. Aframehr, W.; Molki, B.; Heidarian, P.; Behzad, T.; Sadeghi, M.; Bagheri, R. Effect of calcium carbonate nanoparticles on barrier properties and biodegradability of polylactic acid. *Fibers Polym.* **2017**, *18*, 2041–2048. [[CrossRef](#)]
113. Murariu, M.; Dubois, P. PLA composites: From production to properties. *Adv. Drug Deliv. Rev.* **2016**, *107*, 17–46. [[CrossRef](#)] [[PubMed](#)]
114. Chong, W.J.; Shen, S.; Li, Y.; Trinci, A.; Pejak, D.; Kyrtzsis, I.; Sola, A.; Wen, C. Additive manufacturing of antibacterial PLA-ZnO nanocomposites: Benefits, limitations and open challenges. *J. Mater. Sci. Technol.* **2022**, *111*, 120–151. [[CrossRef](#)]
115. Liu, W.; Wu, N.; Pochiraju, K. Shape recovery characteristics of SiC/C/PLA composite filaments and 3D printed parts. *Compos. Part A-Appl. Sci. Manuf.* **2018**, *108*, 1–11. [[CrossRef](#)]
116. Darnal, A.; Shahid, Z.; Deshpande, H.; Kim, J.; Muliana, A. Tuning mechanical properties of 3D printed composites with PLA:TPU programmable filaments. *Compos. Struct.* **2023**, *318*, 117075. [[CrossRef](#)]
117. Yu, F.; Liu, T.; Zhao, X.; Yu, X.; Lu, A.; Wang, J. Effects of talc on the mechanical and thermal properties of polylactide. *J. Appl. Polym. Sci.* **2012**, *125*, E99–E109. [[CrossRef](#)]
118. Yu, W.; Wang, X.; Ferraris, E.; Zhang, J. Melt crystallization of PLA/Talc in fused filament fabrication. *Mater. Des.* **2019**, *182*, 108013. [[CrossRef](#)]
119. Goldschmidt, G.; de Moraes, E.; de Oliveira, A.N.; Hotza, D. Production and characterization of 3D-printed silica-based cellular structures. *Open Ceram.* **2022**, *9*, 100225. [[CrossRef](#)]
120. Ahmed, W.; Siraj, S.; Al-Marzouqi, A.H. 3D Printing PLA Waste to Produce Ceramic Based Particulate Reinforced Composite Using Abundant Silica-Sand: Mechanical Properties Characterization. *Polymers* **2020**, *12*, 2579. [[CrossRef](#)]
121. Travieso-Rodríguez, J.A.; Jerez-Mesa, R.; Llumà, J.; Traver-Ramos, O.; Gomez-Gras, G.; Roa Rovira, J.J. Mechanical Properties of 3D-Printing Polylactic Acid Parts subjected to Bending Stress and Fatigue Testing. *Materials* **2019**, *12*, 3859. [[CrossRef](#)]
122. Monaldo, E.; Ricci, M.; Marfia, S. Mechanical properties of 3D printed polylactic acid elements: Experimental and numerical insights. *Mech. Mater.* **2023**, *177*, 104551. [[CrossRef](#)]
123. Coppola, B.; Cappetti, N.; Di Maio, L.; Scarfato, P.; Incarnato, L. Incarnato; Influence of 3D printing parameters on the properties of PLA/clay nanocomposites. *AIP Conf. Proc.* **2018**, *1981*, 020064. [[CrossRef](#)]
124. Mofokeng, J.P.; Luyt, A.S. Dynamic mechanical properties of PLA/PHBV, PLA/PCL, PHBV/PCL blends and their nanocomposites with TiO₂ as nanofiller. *Thermochim. Acta* **2015**, *613*, 41–53. [[CrossRef](#)]

125. Xu, J.; Xu, F.; Gao, G. The Effect of 3D Printing Process Parameters on the Mechanical Properties of PLA Parts. *J. Phys. Conf. Ser.* **2021**, *2133*, 012026. [[CrossRef](#)]
126. Subramaniyan, M.; Karuppan, S. Mechanical properties of sandwich products obtained by 3D printing from PLA-PLA/Al2O3. *Polimery* **2024**, *68*, 646–651. [[CrossRef](#)]
127. Keshavamurthy, R.; Tambrallimath, V.; Patil, S.; Rajhi, A.A.; Duhduh, A.A.; Khan, T.M.Y. Mechanical and Wear Studies of Boron Nitride-Reinforced Polymer Composites Developed via 3D Printing Technology. *Polymers* **2023**, *15*, 4368. [[CrossRef](#)]
128. Ji, Q.; Wang, Z.; Yi, J.; Tang, X. Mechanical Properties and a Constitutive Model of 3D-Printed Copper Powder-Filled PLA Material. *Polymers* **2021**, *13*, 3605. [[CrossRef](#)]
129. Kumar, S.; Singh, R.; Singh, T.; Batish, A. On mechanical characterization of 3-D printed PLA-PVC-wood dust-Fe3O4 composite. *J. Thermoplast. Compos. Mater.* **2022**, *35*, 36–53. [[CrossRef](#)]
130. Bennett, C.; Sojithamporn, P.; Thanakulwattana, W.; Wattanuchariya, W.; Leksakul, K.; Nakkiew, W.; Jantanasakulwong, K.; Rachtanapun, P.; Suhr, J.; Sawangrat, C. Optimization of 3D Printing Technology for Fabrication of Dental Crown Prototype Using Plastic Powder and Zirconia Materials. *Materials* **2022**, *15*, 8618. [[CrossRef](#)]
131. Luo, X.; Cheng, H.; Wu, X. Nanomaterials Reinforced Polymer Filament for Fused Deposition Modeling: A State-of-the-Art Review. *Polymers* **2023**, *15*, 2980. [[CrossRef](#)]
132. Amza, C.G.; Zapciu, A.; Constantin, G.; Baci, F.; Vasile, M.I. Enhancing Mechanical Properties of Polymer 3D Printed Parts. *Polymers* **2021**, *13*, 562. [[CrossRef](#)] [[PubMed](#)]
133. Camargo, J.C.; Machado, R.; Almeida, E.C.; Silva, E.F.M.S. Mechanical properties of PLA-graphene filament for FDM 3D printing. *Int. J. Adv. Manuf. Technol.* **2019**, *103*, 2423–2443. [[CrossRef](#)]
134. Al Abir, A.; Chakrabarti, D.; Trindade, B. Fused Filament Fabricated Poly(lactic acid) Parts Reinforced with Short Carbon Fiber and Graphene Nanoparticles with Improved Tribological Properties 2019. *Polymers* **2023**, *15*, 2451. [[CrossRef](#)] [[PubMed](#)]
135. Khan, S.; Joshi, K.; Deshmukh, S. A comprehensive review on effect of printing parameters on mechanical properties of FDM printed parts. *Mater. Today Proc.* **2022**, *50 Pt 5*, 2119–2127. [[CrossRef](#)]
136. Zhou, X.; Deng, J.; Fang, C.; Lei, W.; Song, Y.; Zhang, Z.; Huang, Z.; Li, Y. Additive manufacturing of CNTs/PLA composites and the correlation between microstructure and functional properties. *J. Mater. Sci. Technol.* **2021**, *60*, 27–34. [[CrossRef](#)]
137. Patanwala, H.S.; Hong, D.; Vora, S.R.; Bognet, B.; Ma, A.W.K. The microstructure and mechanical properties of 3D printed carbon nanotube-poly(lactic acid) composites. *Polym. Compos.* **2018**, *39*, E1060–E1071. [[CrossRef](#)]
138. Agbakoba, V.C.; Hlangothi, P.; Andrew, J.; John, M.J. Mechanical and Shape Memory Properties of 3D-Printed Cellulose Nanocrystal (CNC)-Reinforced Poly(lactic acid) Bionanocomposites for Potential 4D Applications. *Sustainability* **2022**, *14*, 12759. [[CrossRef](#)]
139. Yang, L.; Li, S.; Zhou, X.; Liu, J.; Li, Y.; Yang, M.; Yuan, Q.; Zhang, W. Effects of carbon nanotube on the thermal, mechanical, and electrical properties of PLA/CNT printed parts in the FDM process. *Synth. Met.* **2019**, *253*, 122–130. [[CrossRef](#)]
140. Podsiadły, B.; Matuszewski, P.; Skalski, A.; Słoma, M. Carbon Nanotube-Based Composite Filaments for 3D Printing of Structural and Conductive Elements. *Appl. Sci.* **2021**, *11*, 1272. [[CrossRef](#)]
141. Jang, H.G.; Yang, B.; Khil, M.-S.; Kim, S.Y.; Kim, J. Comprehensive study of effects of filler length on mechanical, electrical, and thermal properties of multi-walled carbon nanotube/polyamide 6 composites. *Compos. Part A Appl. Sci. Manuf.* **2019**, *125*, 105542. [[CrossRef](#)]
142. Elaskalany, M.; Behdian, K. Effect of carbon nanotube type and length on the electrical conductivity of carbon nanotube polymer nanocomposites. *Mater. Res. Express* **2023**, *10*, 105010. [[CrossRef](#)]
143. Jayanth, N.; Jaswanthraj, K.; Sandeep, S.; Mallaya, N.H.; Siddharth, S.R. Effect of heat treatment on mechanical properties of 3D printed PLA. *J. Mech. Behav. Biomed. Mater.* **2021**, *123*, 104764. [[CrossRef](#)] [[PubMed](#)]
144. Chokshi, H.; Shah, D.B.; Patel, K.M.; Joshi, S.J. Experimental investigations of process parameters on mechanical properties for PLA during processing in FDM. *Adv. Mater. Process. Technol.* **2021**, *8*, 696–709. [[CrossRef](#)]
145. De Bortoli, L.; de Farias, R.; Mezalira, D.; Schabbach, L.; Fredel, M. Functionalized carbon nanotubes for 3D-printed PLA-nanocomposites: Effects on thermal and mechanical properties. *Mater. Today Commun.* **2022**, *31*, 103402. [[CrossRef](#)]
146. Jiang, G.; Yang, T.; Xu, J.; Tao, D.; Luo, C.; Wang, C.; Dong, Q.; Wang, Y. Investigation into hydroxypropyl-methylcellulose-reinforced polylactide composites for fused deposition modelling. *Ind. Crops Prod.* **2020**, *146*, 112174. [[CrossRef](#)]
147. Makri, S.; Xanthopoulou, E.; Klonos, P.; Grigoropoulos, A.; Kyritsis, A.; Tsachouridis, K.; Anastasiou, A.; Deligkiozi, I.; Nikolaidis, N.; Bikiaris, D. Effect of Micro- and Nano-Lignin on the Thermal, Mechanical, and Antioxidant Properties of Biobased PLA-Lignin Composite Films. *Polymers* **2022**, *14*, 5274. [[CrossRef](#)]
148. Gregor-Svetec, D.; Leskovšek, M.; Leskovar, B.; Stanković Elesini, U.; Vrabič-Brodnjak, U. Analysis of PLA Composite Filaments Reinforced with Lignin and Polymerised-Lignin-Treated NFC. *Polymers* **2021**, *13*, 2174. [[CrossRef](#)]
149. Domínguez-Robles, J.; Martin, N.; Fong, M.; Stewart, S.; Irwin, N.; Rial-Hermida, M.; Donnelly, R.; Larrañeta, E. Antioxidant PLA Composites Containing Lignin for 3D Printing Applications: A Potential Material for Healthcare Applications. *Pharmaceutics* **2019**, *11*, 165. [[CrossRef](#)]

150. Liao, J.; Brosse, N.; Pizzi, A.; Hoppe, S.; Zhou, X.; Du, G. Characterization and 3D printability of poly (lactic acid)/acetylated tannin composites. *Ind. Crops Prod.* **2020**, *149*, 112320. [[CrossRef](#)]
151. Liao, J.; Brosse, N.; Hoppe, S.; Zhou, X.; Xi, X.; Du, G.; Pizzi, A. Interfacial improvement of poly (lactic acid)/tannin acetate composites via radical initiated polymerization. *Ind. Crops Prod.* **2021**, *159*, 113068. [[CrossRef](#)]
152. Daver, F.; Lee, K.; Brandt, M.; Shanks, R. Cork–PLA composite filaments for fused deposition modelling. *Compos. Sci. Technol.* **2018**, *168*, 230–237. [[CrossRef](#)]
153. Tao, Y.; Wang, H.; Li, Z.; Li, P.; Shi, S. Development and Application of Wood Flour-Filled Polylactic Acid Composite Filament for 3D Printing. *Materials* **2017**, *10*, 339. [[CrossRef](#)] [[PubMed](#)]
154. Zandi, M.D.; Jerez-Mesa, R.; Lluma-Fuentes, J.; Roa, J.J.; Travieso-Rodriguez, J.A. Experimental analysis of manufacturing parameters' effect on the flexural properties of wood-PLA composite parts built through FFF. *Int. J. Adv. Manuf. Technol.* **2020**, *106*, 3985–3998. [[CrossRef](#)]
155. Åkerlund, E.; Diez-Escudero, A.; Grzeszczak, A.; Persson, C. The Effect of PCL Addition on 3D-Printable PLA/HA Composite Filaments for the Treatment of Bone Defects. *Polymers* **2022**, *14*, 3305. [[CrossRef](#)]
156. Belhassen, R.; Vilaseca, F.; Mutjé, P.; Boufi, S. Thermoplasticized starch modified by reactive blending with epoxidized soybean oil. *Ind. Crops Prod.* **2014**, *53*, 261–267. [[CrossRef](#)]
157. Xiong, Z.; Yang, Y.; Feng, J.; Zhang, X.; Zhang, C.; Tang, Z.; Zhu, J. Preparation and characterization of poly(lactic acid)/starch composites toughened with epoxidized soybean oil. *Carbohydr. Polym.* **2013**, *92*, 810–816. [[CrossRef](#)]
158. Hu, Y.; Gu, J.; Zhang, Y.; Liu, G.; Yi, X.; Liu, X. FDM 3D printed MXene/Recycled carbon fibre reinforced polylactic acid composites: Interface optimization, toughening and enhanced electromagnetic shielding performance. *Compos. Commun.* **2024**, *48*, 101953. [[CrossRef](#)]
159. Vidakis, N.; Kalderis, D.; Michailidis, N.; Papadakis, V.; Mountakis, N.; Argyros, A.; Spiridaki, M.; Moutspoulou, A.; Petousis, M. Environmentally friendly polylactic acid/ferro-nickel slag composite filaments for material extrusion 3D printing: A comprehensive optimization of the filler content. *Mater. Today Sustain.* **2024**, *27*, 100881. [[CrossRef](#)]
160. Zeynivandnejad, M.; Moradi, M.; Sadeghi, A. Mechanical, physical, and degradation properties of 3D printed PLA + Mg composites. *J. Manuf. Process.* **2023**, *101*, 234–244. [[CrossRef](#)]
161. Suvanjumrat, C.; Chansoda, K.; Chookaew, W. Additive manufacturing advancement through large-scale screw-extrusion 3D printing for precision parawood powder/PLA furniture production. *Clean. Eng. Technol.* **2024**, *20*, 100753. [[CrossRef](#)]
162. Yin, Q.; Kong, F.; Wang, S.; Du, J.; Tao, Y.; Li, P. Hazelnut shell carbon filled polylactic acid composite filaments for 3D printing photothermal structures. *J. Mater. Res. Technol.* **2023**, *27*, 3923–3935. [[CrossRef](#)]
163. Ranjan, N.; Kumar, R.; Singh, R.; Ramniwas, S.; Kumar, V. 1.40—On extrusion of PLA-salix alba feedstock filament for scaffolding applications. In *Comprehensive Materials Processing*, 2nd ed.; Saleem, H., Ed.; Elsevier: Amsterdam, The Netherlands, 2024; pp. 367–373. ISBN 9780323960212. [[CrossRef](#)]
164. Fico, D.; Rizzo, D.; De Carolis, V.; Montagna, F.; Palumbo, E.; Corcione, C.E. Development and characterization of sustainable PLA/Olive wood waste composites for rehabilitation applications using Fused Filament Fabrication (FFF). *J. Build. Eng.* **2022**, *56*, 104673. [[CrossRef](#)]
165. Hatkeposhti, J.K.; Kordani, N.; Pasha, M.A.; Barari, A. Fracture load in double keyhole notch PLA-Cu₂O nanocomposites manufactured via compression molding and 3D printing: An experimental and numerical study. *J. Mech. Behav. Biomed. Mater.* **2024**, *153*, 106504. [[CrossRef](#)]
166. Rimpongpisarn, T.; Wattanathana, W.; Sukthavorn, K.; Nootsuwan, N.; Hanlumyuang, Y.; Veranitisagul, C.; Laobuthee, A. Novel luminescent PLA/MgAl₂O₄:Sm³⁺ composite filaments for 3D printing application. *Mater. Lett.* **2019**, *237*, 270–273. [[CrossRef](#)]
167. Qian, Y.; Li, C.; Qi, Y.; Zhong, J. 3D printing of graphene oxide composites with well controlled alignment. *Carbon* **2021**, *171*, 777–784. [[CrossRef](#)]
168. Rahmatabadi, D.; Ghasemi, I.; Baniassadi, M.; Abrinia, K.; Baghani, M. 3D printing of PLA-TPU with different component ratios: Fracture toughness, mechanical properties, and morphology. *J. Mater. Res. Technol.* **2022**, *21*, 3970–3981. [[CrossRef](#)]
169. Ju, Q.; Tang, Z.; Shi, H.; Zhu, Y.; Shen, Y.; Wang, T. Thermoplastic starch based blends as a highly renewable filament for fused deposition modeling 3D printing. *Int. J. Biol. Macromol.* **2022**, *219*, 175–184. [[CrossRef](#)]
170. Yang, J.; Li, W.; Mu, B.; Xu, H.; Hou, X.; Yang, Y. 3D printing of toughened enantiomeric PLA/PBAT/PMMA quaternary system with complete stereo-complexation: Compatibilizer architecture effects. *Polymer* **2022**, *242*, 124590. [[CrossRef](#)]
171. Hui, I.; Pasquier, E.; Solberg, A.; Agrenius, K.; Håkansson, J.; Chinga-Carrasco, G. Biocomposites containing poly(lactic acid) and chitosan for 3D printing—Assessment of mechanical, antibacterial and in vitro biodegradability properties. *J. Mech. Behav. Biomed. Mater.* **2023**, *147*, 106136. [[CrossRef](#)]

Disclaimer/Publisher's Note: The statements, opinions and data contained in all publications are solely those of the individual author(s) and contributor(s) and not of MDPI and/or the editor(s). MDPI and/or the editor(s) disclaim responsibility for any injury to people or property resulting from any ideas, methods, instructions or products referred to in the content.